

DETERMINATION OF THE ROLE OF PLASMALOGENS IN
THE MYELINATION PROCESS AND MYELIN MAINTENANCE

JESSICA FARIA DA EIRA

Dissertação de Mestrado em Bioquímica

Universidade do Porto

Faculdade de Ciências

Instituto de Ciências Biomédicas Abel Salazar

2012

JESSICA FARIA DA EIRA

**DETERMINATION OF THE ROLE OF
PLASMALOGENS IN THE MYELINATION
PROCESS AND MYELIN MAINTENANCE**

Dissertação de Candidatura ao grau de Mestre em
Bioquímica da Universidade do Porto

Orientador – Doutor Pedro Brites

Categoria – Post-Doc

Afiliação – Instituto de Biologia Molecular e Celular

2012

AGRADECIMENTOS

Considerando o facto de que o trabalho que eu desenvolvi neste período da minha formação académica foi apenas possível graças à colaboração de várias pessoas, gostaria de exprimir, deste modo, o meu agradecimento a todos os que me deram um incentivo nos momentos certos. Assim, gostaria de agradecer:

- Ao Doutor Pedro Brites, meu orientador, por me ter aceitado nesta Tese de Mestrado e pela sua dedicação como orientador, tal como pelo apoio e pelos ensinamentos oferecidos ao longo deste ano.
- À Doutora Mónica Sousa por me ter aceitado no laboratório de Regeneração Nervosa permitindo-me estender os meus conhecimentos nesta área e ao Tiago Silva, bem como a todo o grupo de Regeneração Nervosa, pela ajuda e assistência prestada em todas as minhas dúvidas e dificuldades ao longo do ano.
- À comissão de curso de Bioquímica por me ter aceitado como aluna no curso de Mestrado em Bioquímica, nomeadamente à Doutora Maria João Saraiva pela disponibilidade e dedicação prestadas como minha tutora na Tese de Mestrado.
- Aos meus amigos de mestrado por todos os momentos de companheirismo que tornaram estes dois anos extremamente agradáveis e inesquecíveis. Ao resto dos meus amigos pela paciência e compreensão em todos os momentos em que os deixei para trás ao longo destes dois anos.
- Finalmente, à minha família por sempre me terem apoiado e encorajado no prosseguimento dos meus objectivos, especialmente ao Marcelo, Carina e Gabriel por nunca me terem recusado apoio e aos meus pais por toda a paciência e dedicação e porque sem eles isto nunca teria sido possível.

ABSTRACT

Plasmalogens are a class of ether-phospholipids with fundamental structural and functional roles in biological membranes. They are distributed throughout different tissues albeit in varied proportions, being the nervous tissue particularly rich in these phospholipids. The biosynthetic pathway of plasmalogens occurs in a bi-localized manner. The first two steps occur in the peroxisome and the remaining in the endoplasmic reticulum. Therefore, syndromes which have the assembly of peroxisomes compromised generate an impairment in plasmalogen biosynthesis which leads to a deficiency in plasmalogens. Rhizomelic chondrodysplasia punctata (RCDP), a peroxisomal disorder caused by deficiency in the biosynthesis of plasmalogens, highlights the importance of plasmalogens in multiple tissues, as the patients present cataracts, abnormal endochondral ossification, hypotonia and mental retardation. As reduced plasmalogen levels have been observed in neurodegenerative disorders (e.g. X-linked adrenoleukodystrophy and Alzheimer's disease) it is of special importance to understand the consequences and functions of these phospholipids in nervous tissue.

Using two mouse models with a complete impairment in the plasmalogens biosynthesis pathway (Pex7 and Gnpat knockout mice (KO)) we determined the importance of plasmalogens in myelination and the consequences of a plasmalogen deficiency in the peripheral nervous system.

Results obtained showed that the absence of plasmalogens affects myelination and radial sorting. As hypomyelination was a feature in the nerves of young KO mice, we also characterized myelin and Schwann cell morphology in adult mice. Our results show that in the absence of plasmalogens and despite normal amounts, myelin is abnormally formed with an increase in non-compact myelin (higher number of Schmidt Lanterman incisures) and incorrect compartmentalization of the Schwann cell cytoplasm. In aged KO mice, the lack of plasmalogens causes a severe demyelination and axonal loss. Evaluations of the molecular mechanisms behind the defect in myelination demonstrated a defect in the AKT-mediated signalling pathway due to an impairment in AKT recruitment to the plasma membrane. By unravelling the pathology and the mechanism of disease, we were able to devise and determine the effectiveness of a therapeutic strategy aimed at inhibiting GSK3 β , a downstream effector of the AKT-mediated signalling pathway.

Using lithium, a well known GSK3 β inhibitor, we showed that there was a rescue of the defective radial sorting and myelination.

Combined, our results unravelled a new role of plasmalogens in cellular biology, characterized the pathology caused by a deficiency in plasmalogens and determined the mechanisms behind it. Future work should include the determination if a lithium treatment may have beneficial effects in adult knockout mice or if combined therapies have a truly therapeutic potential.

Keywords: AKT; ether-phospholipids; Gnpat; myelination; mouse knockout; plasmalogens; PNS; radial sorting; rhizomelic chondrodysplasia punctata; Schwann cell; therapy

RESUMO

Os plasmalogénios são uma classe de éter fosfolípidos com funções estruturais e funcionais fundamentais nas membranas biológicas. Estes encontram-se distribuídos em vários tecidos embora que em variadas proporções, sendo o tecido nervoso particularmente rico nestes fosfolípidos. Na via biossintética dos plasmalogénios, os primeiros dois passos dão-se no peroxissoma e os restantes no retículo endoplasmático. Deste modo, síndromes onde a formação dos peroxissomas esteja comprometida levam a um défice de plasmalogénios por um bloqueio na sua biossíntese. A Condrodisplasia Rizomélica punctata (CDRP), uma doença peroxissomal causada por uma deficiência na biossíntese de plasmalogénios, realça a importância dos plasmalogénios em variados tecidos, uma vez que os pacientes apresentam cataratas, defeitos na ossificação endocondral, hipotonia e atraso mental. Uma vez que níveis reduzidos de plasmalogénios têm sido observados em doenças neurodegenerativas (ex. Adrenoleucodistrofia ligada ao cromossoma X e doença de Alzheimer), é de especial importância entender as consequências e as funções destes fosfolípidos no tecido nervoso.

Utilizando dois modelos de ratinho com um dano completo na via biossintética de plasmalogénios (ratinhos *Pex7* e *Gnpat knockout* (KO)), investigámos a importância dos plasmalogénios na mielinização e as consequências da deficiência destes no sistema nervoso periférico.

Os resultados obtidos demonstraram que a ausência de plasmalogénios afecta a mielinização e o *radial sorting*. Dado que nós observámos uma hipomielinização em nervos ciáticos de ratinhos KO jovens também se caracterizou a morfologia da mielina e da célula de Schwann em ratinhos adultos. Os resultados demonstraram que na ausência de plasmalogénios e apesar dos valores normais de mielina, esta foi formada anormalmente pois possuía um aumento em mielina não compacta (aumento no número de incisuras de Schmidt Lanterman) e uma compartimentalização incorrecta do citoplasma da célula de Schwann. Em ratinhos KO envelhecidos, a ausência de plasmalogénios mostrou provocar uma demielinização pronunciada e perda axonal. A determinação dos mecanismos moleculares associados ao defeito na mielinização observado demonstraram um defeito na activação da via de sinalização mediada por AKT devido a um recrutamento defeituoso da AKT para a membrana plasmática. Desvendando a

patologia e o mecanismo da doença, foi-nos permitido desenhar e determinar a eficácia de uma estratégia terapêutica consistindo na inibição da GSK3 β , um efector que se encontra na base da via de sinalização mediada pela AKT. Utilizando Lítio, um conhecido inibidor da GSK3 β , demonstrou-se que existe uma recuperação na deficiência na mielinização e no *radial sorting*.

Combinados, os nossos resultados desvendaram um novo papel dos plasmalogénios na biologia celular, permitiram a caracterização da patologia causada por uma deficiência em plasmalogénios e a determinação dos mecanismos por trás desta deficiência. Trabalho futuro deveria determinar se o tratamento com Lítio poderá ter efeitos benéficos em ratinhos KO adultos ou se terapias combinadas poderão ter verdadeiramente um potencial terapêutico.

Palavras chave: AKT; Célula de Schwann; condrodissplasia rizomélica punctata; éter-fosfolípidos; Gnpat; mielinização; plasmalogénios; *radial sorting*; ratinho *knockout*; SNP; terapia

TABLE OF CONTENTS

AGRADECIMENTOS	III
ABSTRACT	V
RESUMO	VII
ABBREVIATIONS LIST	1
FIGURES LIST	5
TABLES LIST	6
CHAPTER I - INTRODUCTION.....	9
PHOSPHOLIPIDS	11
PLASMALOGENS	12
PLASMALOGENS' BIOSYNTHETIC PATHWAY	13
PLASMALOGENS' BIOLOGICAL AND PHYSIOLOGICAL FUNCTIONS.....	15
PLASMALOGENS IN DISEASE.....	17
Zellweger Syndrome (ZS).....	18
Rhizomelic Chondrodysplasia punctata (RCDP)	18
Alzheimer's Disease (AD)	20
Niemann Pick Type C Disease (NPC).....	20
PLASMALOGEN DEFICIENT MICE MODELS	21
Pex7 knockout mouse model	21
Gnpat knockout mouse model.....	22
PERIPHERAL NERVOUS SYSTEM MYELIN SYNTHESIS AND STRUCTURE.....	23
Schwann cell and PNS myelin synthesis	23
PNS axonal and Schwann cell structure and composition	25
REGULATION OF PNS MYELINATION – MOLECULAR MECHANISMS	28
PLASMALOGENS IN NERVOUS TISSUE.....	30
CHAPTER II - AIMS OF THE THESIS.....	31
CHAPTER III - MATERIALS AND METHODS.....	35
ANIMAL HANDLING AND MOUSE MODELS	37

Pex7 and Gnpat knockout mice models	37
LiCl treatment	37
HISTOLOGICAL ASSESSMENT OF SCIATIC NERVES	38
Sciatic nerve fixation and processing	38
Morphometric assessment of sciatic nerve from 17 months old mice	38
Morphometric assessment of sciatic nerve from LiCl treated mice	39
Teased Fibers	39
IN VITRO MYELINATION ASSAY	39
<i>in vitro</i> Myelination Assay with LiCl Treatment	40
CELL CULTURE.....	41
Mouse embryonic fibroblasts (MEFs) culture	41
FBS stimulation of MEFs	41
BIOCHEMICAL ASSESSMENT.....	41
Sample Preparation and Western Blotting.....	41
Subcellular Fractionation.....	42
STATISTICAL ANALYSIS	43
CHAPTER IV - RESULTS.....	45
DEMYELINATION IN THE ABSENCE OF PLASMALOGENS	48
DISORGANIZED MYELIN IN THE ABSENCE OF PLASMALOGENS	51
DEFECTIVE MYELINATION IN THE ABSENCE OF PLASMALOGENS	53
IMPAIRED SIGNALLING PATHWAYS DURING MYELINATION PROCESS	55
DEFICIENT AKT PATHWAY ACTIVATION IN PLASMALOGEN ABSENCE	57
LACK OF PLASMALOGENS IMPAIRS MEMBRANE RECRUITMENT OF AKT	59
INHIBITION OF GSK3 β RESCUES PNS DEFECTS OF PLASMALOGEN-DEFICIENCY	60
CHAPTER V - DISCUSSION.....	67
CHAPTER VI - CONCLUSIONS.....	75
REFERENCES	79

ABBREVIATIONS LIST

AA	Ascorbic acid
AADHAP-R	Acyl/alkyl-dihydroxyacetone phosphate reductase
AAG3P-AT	Alkyl/acyl-glycero-3-phosphate acyltransferase
ACAA1	3-oxoacyl-CoA thiolase
AD	Alzheimer's disease
ADHAP-S	Alkyl-dihydroxyacetone phosphate synthase
Agps	Alkylglycerone phosphate synthase
BSA	Bovine serum albumine
Ca ²⁺	Calcium ion
Caspr	Contactin associated protein
CDRP	Condrodisplasia rizomélica punctata
CNS	Central Nervous System
C-PT	Choline Phosphotransferase
DHAP	Dihydroxyacetone phosphate
DHAP-AT	Dihydroxyacetone phosphate acyltransferase
DMEM	Dulbecco's modified eagle medium
DNA	Deoxyribonucleic acid
DRG	Dorsal root ganglion
DRP2	Dystrophin related protein 2
E(x)	Embryonic day (x)
EDTA	Ethylenediaminetetraacetic acid
EM	Electron Microscopy
E-PT	Ethanolamine Phosphotransferase
ER	Endoplasmic reticulum
ErbB2	Erythroblastic Leukemia Viral Oncogene Homolog 2
ErbB3	Erythroblastic Leukemia Viral Oncogene Homolog 3
Erk1/2	Extracellular signal regulated kinase 1/2
f-actin	Filamentous actin
FBS	Fetal bovine serum
G3P	Glycerol-3-phosphate
GAPDH	Glyceraldehyde 3-phosphate dehydrogenase
Gnpat	Glycerone-phosphate O-acyltransferase

GPC	Glycero-3-phosphocholine
GPE	Glycero-3-phosphoethanolamine
GSK3 β	Glycogen synthase kinase 3 β
GTA	Glutaraldehyde
ICC	Immunocytochemistry
Jnk	c-Jun N-terminal kinase
KO	Knockout
Krox20	Erg2 - early growth response
LiCl	Lithium chloride
LRM	Lipid raft microdomain
MBP	Myelin basic protein
MEFs	Mouse embryonic fibroblasts
MF	Myelinated Fibre
MRI	Magnetic resonance imaging
Na ⁺	Sodium ion
NaCl	Sodium chloride
NDS	Normal Donkey Serum
NFATc4	Nuclear factor of activated T-cells
NFDM	Non-fat dry milk
NGF	Nerve growth factor
NPC	Niemann Pick Type C Disease
NRG1-III	Neuregulin-1 type III
O/N	Over-night
Oct6	Octamer-binding transcription factor-6
OD	Optical density
P(x)	Post natal day (x)
P/S	Penicillin/Streptomycin
P0	Myelin protein zero
PAF	Platelet activating factor
PBD	Peroxisomal biogenesis disorder
PBS	Phosphate buffered saline pH 7.6
PC-plasmalogen	Plasmenylcholine plasmalogen
PE-plasmalogen	Plasmenylethanolamine plasmalogen
Pex7	Peroxin 7
PFA	Paraformaldehyde

PH	Phosphohydrolase
PhyH	Phytanoyl-CoA hydroxylase
PI3K	Phosphatidylinositol 3-kinase
PIP3	Phosphatidylinositol (3,4,5)-triphosphate
PLC-γ	Phospholipase C-γ
PNS	Peripheral Nervous System
PPD	p-phenylenediamine
PsPLA2	Plasmalogen specific phospholipase A2
PTEN	Phosphatase and tensin homologue
PTS1	Peroxisomal targeting signal 1
PTS2	Peroxisomal targeting signal 2
PUFA	Polyunsaturated fatty acid
RCDP	Rhizomelic Chondrodysplasia punctata
ROS	Reactive Oxygen Species
RT	Room temperature
RTK	Receptor tyrosine kinase
SC	Schwann cell
SDS-PAGE	Sodium dodecyl sulfate polyacrylamide gel electrophoresis
Ser	Serine
SLI	Schmidt Lanterman Incisures
SNP	Sistema nervoso Periférico
Sox10	SRY-related HMG-box10
Sox2	SRY-related box2
Stat3	Signal transducer and activator of transcription 3
TBS	Tris-buffered saline
Thr	Threonine
Tyr	Tyrosine
VLCFA	Very long chain fatty acid
WB	Western Blot
WT	Wild-type
Yy1	Yin yang-1
ZS	Zellweger Syndrome

FIGURES LIST

FIGURE 1. OVERVIEW OF THE STRUCTURE OF GLYCEROPHOSPHOLIPIDS.	11
FIGURE 2. REPRESENTATIVE ILLUSTRATION OF THE PLASMALOGENS' BIOSYNTHETIC PATHWAY..	14
FIGURE 3. FUNCTIONS PROPOSED FOR PLASMALOGENS <i>VERSUS</i> THE PROCESSES AFFECTED WITH THEIR ABSENCE FROM THE MEMBRANES.	16
FIGURE 4. THE SCHWANN CELL DEVELOPMENT PROCESS IN MOUSE, SCHEMATIC ILLUSTRATION OF THE MAIN CELL TYPES AND DEVELOPMENTAL TRANSITIONS IN SCHWANN CELL.	24
FIGURE 5. STRUCTURE OF A PNS MYELINATED AXON AND THE MOLECULAR COMPOSITION IN THE DIFFERENT NODAL REGIONS.	26
FIGURE 6. SCHEMATIC REPRESENTATION OF THE SCHWANN CELL MEMBRANE COMPARTMENTS.	27
FIGURE 7. TRANSCRIPTIONAL REGULATION OF MYELINATION IN THE PNS.	29
FIGURE 8. REPRESENTATIVE SCHEME DESCRIBING THE LiCl TREATMENT STRATEGY.	38
FIGURE 9. REPRESENTATIVE SCHEME OF THE <i>IN VITRO</i> MYELINATION ASSAY.	40
FIGURE 10. CONSEQUENCES OF PLASMALOGEN DEFICIENCY TO PNS.	47
FIGURE 11. DEFICIENCY IN MYELIN MAINTENANCE IN THE ABSENCE OF PLASMALOGENS DEMONSTRATED BY AN AGE-DEPENDENT DEMYELINATION.....	48
FIGURE 12. ABSENCE OF PLASMALOGENS LEADS TO AXON LOSS AND DEMYELINATION..	49
FIGURE 13. SCIATIC NERVES FROM PLASMALOGEN DEFICIENT MICE EXHIBIT AXON LOSS, DEMYELINATION AND FAILURE TO REMYELINATE.	50
FIGURE 14. MYELIN STRUCTURE AND COMPOSITION IS ALTERED IN THE ABSENCE OF PLASMALOGENS.	51
FIGURE 15. PLASMALOGEN DEFICIENCY LEADS TO ABNORMAL MYELIN IN STRUCTURE.....	52
FIGURE 16. DEFECTIVE <i>IN VITRO</i> MYELINATION IN THE ABSENCE OF PLASMALOGENS.	54

FIGURE 17. PLASMALOGEN DEFICIENCY DOES NOT AFFECT THE ACTIVATION OF JNK, STAT3 AND ERK1/2.	56
FIGURE 18. PLASMALOGEN DEFICIENT MICE SHOW AN ALTERED PHOSPHORYLATION STATUS OF AKT AND TWO OF ITS DOWNSTREAM TARGETS, GSK3 β AND C-RAF.	56
FIGURE 19. ABSENCE OF PLASMALOGENS INTERFERES WITH AKT ACTIVATION IN GNPAT KO MEFs.....	58
FIGURE 20. PLASMALOGEN DEFICIENCY LEADS TO IMPAIRED RECRUITMENT OF AKT TO THE PLASMA MEMBRANE.	59
FIGURE 21. LICL TREATMENT IS ABLE TO REVERT THE DEFECT IN MYELINATION IN PLASMALOGEN DEFICIENT MICE.....	61
FIGURE 22. LICL RESTORES AKT ACTIVATION AND GSK3 β INHIBITION IN GNPAT KO MICE.....	62
FIGURE 23. LICL TREATMENT INACTIVATES GSK3 β IN THE PERIOD OF AXONAL SORTING.....	63
FIGURE 24. LICL TREATMENT RESTORES SCHWANN CELL DIFFERENTIATION.....	64
FIGURE 25. LICL TREATMENT RESCUES RADIAL SORTING AND MYELINATION.....	65
FIGURE 26. SUMMARIZED MODEL REPRESENTING THE PATHOLOGY AND MECHANISMS INHERENT TO PLASMALOGEN DEFICIENCY.....	74

TABLES LIST

TABLE 1. REPRESENTATION OF PLASMALOGEN DISTRIBUTION IN HUMAN CELLS AND TISSUES.	13
TABLE 2. SUMMARIZED LIST OF ANTIBODIES USED IN THIS WORK.....	43

CHAPTER I

INTRODUCTION

PHOSPHOLIPIDS

Lipids are a class of organic molecules with well described and very important biological functions. The nervous system is reliant on the roles of specific phospholipids which may act as structural components of myelin and may also incorporate the mediation of signalling processes.

Glycerophospholipids constitute a subclass of phospholipids and represent the majority of the lipid content in biological membranes. Structurally, they contain fatty acid ester linkages at *sn1* and *sn2* positions (Figure 1A) [1].

A special class of glycerophospholipids are the ether linked glycerophospholipids that contain an ether linked to the *sn1* position rather than an ester (Figure 1 B). In a general way, ether glycerophospholipids consist of a glycerol backbone which contains attached at the *sn-1* and *sn-2* positions long fatty acid chains and attached to the *sn-3* position is a varying polar head group [2].

At the *sn-1* position there are two types of ether bonds that may occur in these ether-phospholipids: the ether bond, mentioned previously, which is present in platelet activating factor (PAF) and the vinyl-ether bond occurring in plasmalogens (Figure 1 C) [3].

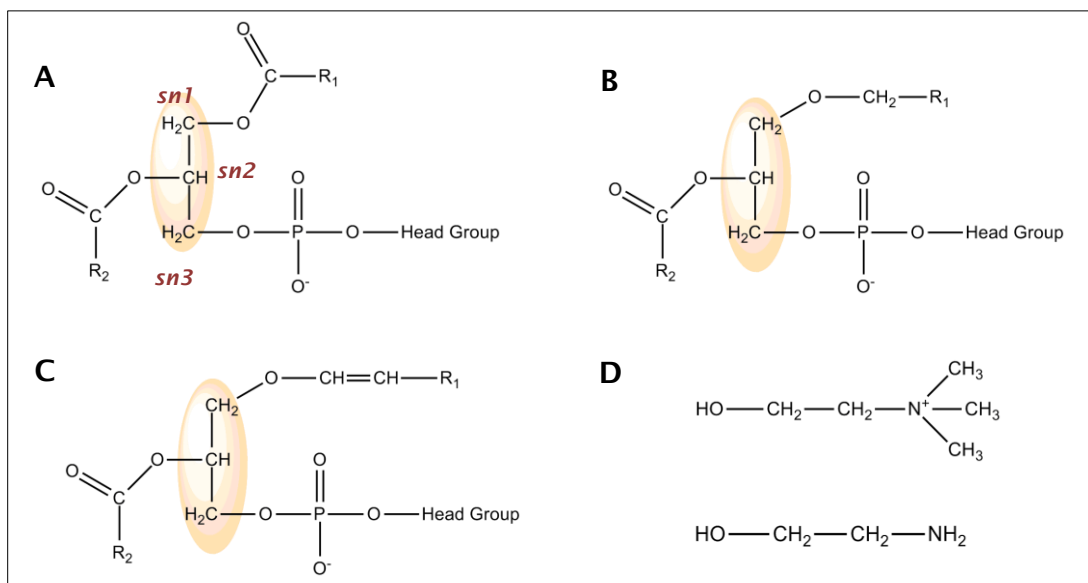


Figure 1. Overview of the structure of Glycerophospholipids. Represented in the image is the structure of a glycerophospholipid (A), an ether-glycerophospholipid (B) and a vinyl-ether glycerophospholipid (C) also known as Plasmalogen. Plasmalogens may have one of two different head groups: choline or ethanolamine (D). Highlighted is the glycerol backbone. Adapted from [3], [4].

Plasmalogens (1-O-alk-1'-enyl-2-acyl glycerophospholipids) belong, as described above, to a subclass of ether phospholipids and are characterized by the presence of a *cis* double bond on the alkyl chain adjacent to the ether linkage at the *sn*-1 position giving rise to the characteristic vinyl-ether bond [2], [3], [5].

These vinyl-ether phospholipids were first described in 1924 by Feulgen and Voit [6] when they discovered during a routine nuclear staining technique a lipidic compound which was insoluble in water but easily extracted with organic solvents. They verified that in the presence of acid or mercuric chloride, the then unknown substance suffered a reaction which led to the formation of an aldehyde as it was stained with fuchsin-sulfurous acid. This substance known to be an aldehyde was named "*plasma*" since it was present in the plasma and the termination was due to its aldehyde nature. The precursor was named "*plasmalogen*" owed to its capacity to generate "*plasma*" [6].

Plasmalogens have a very well characterized and defined structure in which the *sn*-1 position is usually occupied by a 16:0 (palmitic acid), 18:0 (stearic acid) or 18:1 (oleic acid) carbon chain, the *sn*-2 position is occupied by a polyunsaturated fatty acid (PUFA) and the *sn*-3 is occupied by one of the two polar head groups: ethanolamine or choline which give rise to plasménylethanolamine and plasménylcholine plasmalogens respectively [3]. These two types of plasmalogens exist in human tissues in different proportions where PE-plasmalogen is in general more abundant than PC-plasmalogen with exception of the heart muscle where PC-plasmalogen dominates in abundance [7].

The distribution of plasmalogens among living organisms is extensive and they are present in anaerobic bacteria, some fungi, higher plants, invertebrates and vertebrates, including mammals and man [8], [9]. They play important roles in the function and structure maintenance of biological membranes [3], [5], [10], [11], as well as in the storage of long chain polyunsaturated fatty acids (PUFAs), ion transport [12], [13] and lipid secondary messenger genesis [10].

Regarding mammalian tissues, they are widely abundant and consist of approximately 18% of the total phospholipid content in humans. The relative amount and composition of plasmalogens varies among the different tissues, being these ether-phospholipids more abundant in the brain, heart, inflammatory cells and spermatozoa (table 1) [2]. Plasmalogens' distribution varies depending

on the species [9]. Furthermore, regarding its topology, plasmalogens have an asymmetric distribution in biological membranes [14]. PE-plasmalogens are mostly found in the inner leaflet of the plasma membrane such as in the case of sarcolemmal membrane, in red blood cells and myelin [14], [15], [16].

Table 1. Representation of plasmalogen distribution in human cells and tissues. Human brain, heart, inflammatory cells and spermatozoa are particularly rich in these ether-phospholipids. Adapted from [10] and [2].

Tissues /Cells	Human Heart	Human Brain	Inflammatory cells	Human Plasma	Human Spermatozoa	Human Kidney	Human Lungs
	32-50 %	20-50 %	Up to 50 %	5 %	55 %	20-40 %	20-40 %

PLASMALOGENS' BIOSYNTHETIC PATHWAY

The plasmalogens' biosynthetic pathway starts with the action of the enzyme dihydroxyacetone phosphate acyltransferase (DHAP-AT) also known as glycerone-phosphate O-acyltransferase (Gnpat) where the esterification of dihydroxyacetone phosphate (DHAP) with an acyl-CoA ester leads to the formation of 1-acyl-DHAP (Figure 2). The second step of the biosynthetic pathway involves the introduction of the ether bond at the *sn*-1 position. At this point, alkyl-dihydroxyacetone phosphate synthase (ADHAP-S) also known as alkylglycerone phosphate synthase (Agps) replaces the fatty acid at the *sn*-1 position by a fatty alcohol yielding 1-alkyl-DHAP [3].

There are different possibilities for the origin of these fatty alcohols. On one hand they may be derived from dietary sources in the form of wax esters found in fish and vegetables [17], [18]. Other possibility is the reduction of fatty acids such as acyl-CoA chains catalysed by fatty acyl-CoA reductase [19], [20]. One third explanation for the origin of the fatty alcohol focuses on the peroxisomal β -oxidation with chain elongation of dodecanoyl-CoA inside this organelle [21].

The third enzyme involved in the pathway is acyl/alkyl-dihydroxyacetone phosphate reductase (AADHAP-R) which has the function of reducing the ketone group at the *sn*-2 position in the glycerol backbone. The product of this reaction

is 1-alkyl-*sn*-glycero-3-phosphate which is subsequently acylated to 1-alkyl-2-acyl-*sn*-glycero-3-phosphate by alkyl/acyl-glycero-3-phosphate acyltransferase (AAG3P-AT). The next step consists in the removal of the phosphate group by a phosphohydrolase (PH) originating 1-alkyl-2-acyl-*sn*-glycerol. The cytidine-diphosphate-ethanolamine (CDP-ethanolamine) group is integrated through the action of ethanolamine phosphotransferase leading to the formation of 1-alkyl-2-acyl-*sn*-glycero-3-phosphoethanolamine (1-alkyl-2-acyl-GPE). The last step in the formation of PE-plasmalogen consists in a desaturation reaction performed by a Δ^1 -alkyl desaturase and a cytochrome *b5*-dependent microsomal electron transport system. Finally, the PC-plasmalogen formation occurs from PE-plasmalogen through head group transformations, namely via a hydrolytic exchange mechanism [22].

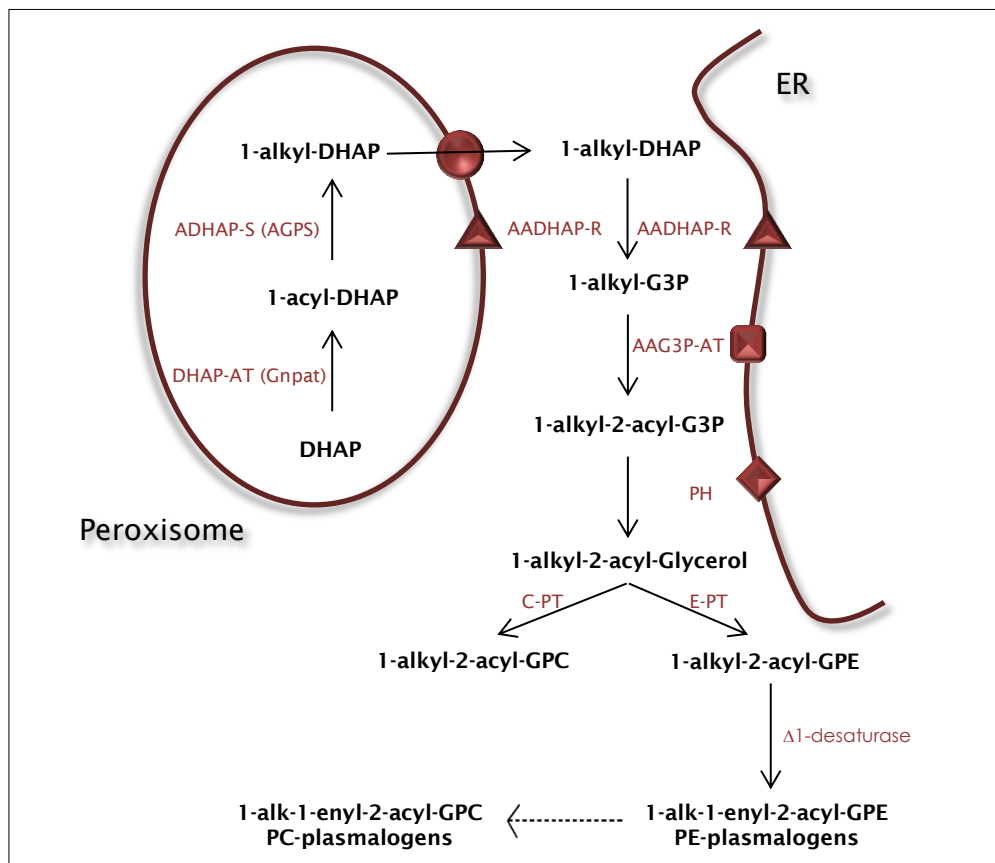


Figure 2. Representative illustration of the plasmalogens' biosynthetic pathway. The first two steps occur exclusively in the peroxisome, the third step presents a bimodal localization being able to occur either on the external surface of the peroxisomal membrane or in the ER (Endoplasmic reticulum). The remaining biosynthetic pathway occurs in the ER. Adapted from [4].

The plasmalogens' biosynthetic pathway is divided into two subcellular compartments. The first two reactions take place in the peroxisome since the

enzymes DHAP-AT and ADHAP-S have exclusive peroxisomal localization. The third step in this biosynthetic pathway has a bi-localized character as AADHAP-R has been described as having bimodal localization, being present in the peroxisomal membrane facing the cytosol and in the Endoplasmic Reticulum (ER). The remaining pathway occurs in the ER [2], [23].

PLASMALOGENS' BIOLOGICAL AND PHYSIOLOGICAL FUNCTIONS

Plasmalogens are important constituents of plasma membrane presenting themselves in varying but significant amounts depending on the tissue. Deficiency in these ether-phospholipids leads to an impairment in the membrane's structure and functions. These impairments were demonstrated by experiments on plasmalogen deficient cells (usually skin fibroblasts) which reported decreased membrane intra- and extra-cellular cholesterol transport, impaired membrane traffic and impaired vesicular function [4].

Plasmalogens are included in the lipid mediation process as they serve as providers of arachidonic acid and docohexanoic acid and consequently as a reservoir of lipid secondary messengers. Plasmalogens are metabolized by a plasmalogen specific phospholipase A₂ (psPLA₂) which leads to the formation of lysoplasmalogens and the release of an aldehyde from the *sn*-1 position. Arachidonic and docohexanoic acid are released from the *sn*-2 position of plasmalogens through the action of a phospholipase, entering the eicosanoid formation pathway and the generation of the first wave of secondary messengers. Moreover, lysoplasmalogens exhibit the ability to increase membrane permeability allowing Ca²⁺ influx and generating a succeeding wave of secondary messenger response [24], [25]. These functions are intricately associated with an additional plasmalogen's function where it acts as an important PUFA storage agent [3], [26], [12] that leads to the eicosanoids production such as prostaglandins and leukotrienes [4].

Regarding the involvement of plasmalogens in membrane dynamics, it is important to refer their involvement with lipid raft microdomains (LRMs). LRMs are specialized regions of the cell membrane particularly rich in cholesterol, glycosphingolipids and specific proteins involved in signal transduction, thence

being associated as important membrane regions of cellular signalling [27]. Due to their signalling functions, these LRMs are distinct from the rest of the cellular membrane concerning membrane fluidity and according to Pike *et al.* [28] ethanolamine plasmalogens are particularly abundant in these regions. This finding suggests a role for plasmalogens in the modulation of the membrane fluidity in lipid rafts [4], [27], [11].

Plasmalogens are also described as scavengers of reactive oxygen species and as antioxidant agents [29]. The presence of the acid-labile vinyl-ether bond which characterizes plasmalogens contributes to their susceptibility to oxidative attack in contrast to diacylphospholipids [30]. So, plasmalogens are able to use their ether-bond as bait acting as scavengers and protecting other phospholipids from oxidative damage [3]. Experiments using plasmalogen deficient cells from patients with peroxisomal biogenesis disorders (PBDs) showed an increase in the sensitivity to UV radiation exposure [31]. In addition, in normal cells, upon exposure to high oxidative conditions, the plasmalogen levels decrease, corroborating the possible function as scavengers [32].

Taking all this, plasmalogens are associated to several biological functions which will have impact in different cellular processes (Figure 3).

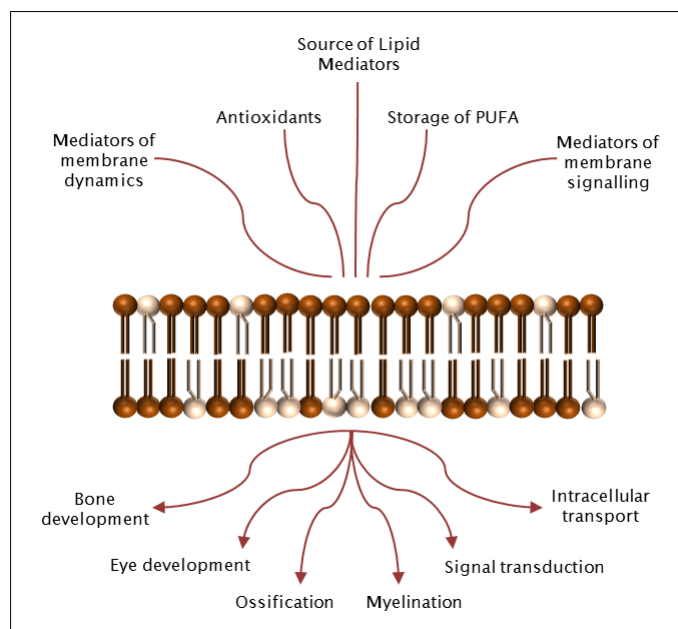


Figure 3. Functions proposed for plasmalogens versus the processes affected with their absence from the membranes. Plasmalogens are described to have several biological functions such as antioxidant activity, mediation of membrane dynamics and membrane signalling, among others. Furthermore, many biological functions are impaired with their absence such as bone and eye development, myelination and others. Plasmalogens are represented in this membrane as the beige phospholipid while the diacylphospholipid are represented in brown. Figure adapted from [3].

PLASMALOGENS IN DISEASE

In the past decades, plasmalogens have been reported to be involved in the pathology of several human disorders. The fact that plasmalogen levels are altered in several human disorders, leads to the deliberation that these ether phospholipids may play an important role in these diseases.

As previously referred, plasmalogens have a variety of biological functions that, when impaired, give rise to deficiencies in a number of physiological processes. There are some descriptions about plasmalogens' roles in spermatogenesis and eye development. Spermatozoa are rich in ether phospholipids namely PC and PE plasmalogens. An important role of plasmalogens in the spermatogenic process was demonstrated both with Pex7 [33] and Gnpat [5], [34] knockout mouse models in which testis from these mouse models demonstrated an arrested spermatogenic process, disorganized seminiferous tubules and infertility. Plasmalogens are also intricately involved in lens development demonstrated also with Gnpat [5] knockout mouse models. Plasmalogen deficiency leads to impaired anterior lens epithelial cell polarity and bilateral cataract [34]. Besides the ones referred above, there are several other roles associated to plasmalogens namely in the ossification [35] and myelination process [36].

In a general way, plasmalogen deficiency associated human disorders are linked with an impaired peroxisomal biogenesis or function [2]. In fact, PBDs lack plasmalogens since the two first steps of the biosynthetic pathway occur exclusively in the peroxisome (Figure 2).

According to Nagan and Zoeller [2], disorders that lead to plasmalogen deficiency because of the absence of peroxisomes or lack of their function can be divided into three groups:

- Group A disorders that are characterized by a generalized loss of peroxisomes (eg. Zellweger syndrome and Neonatal X-linked adrenoleukodystrophy);
- Group B disorders that present the inability to target peroxisomal proteins to the peroxisome (eg. Rhizomelic chondrodysplasia punctata type 1);
- Group C disorders that display a defect on a single peroxisomal enzyme or function (eg. Rhizomelic chondrodysplasia punctata type 2 and 3);

ZELLWEGER SYNDROME (ZS)

ZS is considered the prototype of the group of peroxisomal diseases [37] and is defined as an autosomal recessive neonatal neurodegenerative disorder in which the peroxisome biogenesis is compromised leading to a generalized lack of peroxisomes [4]. Clinically, Zellweger syndrome patients exhibit craniofacial dysmorphism, hypotonia, growth retardation and neurological abnormalities [3]. Biochemically, there is an accumulation of very long chain fatty acids (VLCFA), bile acid intermediates, phytanic acid and pristanic acid, as well as reduced plasmalogen content [3], [37]. Regarding brain pathology, ZS patients display dysmyelination rather than demyelination and neuronal migration defects [37], which leads to the suggestion that the reduced levels of plasmalogens in the brain tissue in this syndrome may have a consequence in the neuronal migration and myelination abnormalities [38]. Observations that membrane fluidity is higher in Zellweger syndrome patients cells strengthens the idea that plasmalogens may be involved in membrane dynamics and also signal transduction [11].

RHIZOMELIC CHONDRODYSPLASIA PUNCTATA (RCDP)

RCDP is an autosomal recessive peroxisomal disorder characterized by distinct pathological and biochemical features and a very short life expectancy [39].

Biochemically, it is characterized by an impairment in plasmalogens and other ether phospholipids synthesis [40], [41] mostly because the activity and expression levels of the two enzymes responsible for the *de novo* synthesis of plasmalogens - Gnpat and Agps - are severely compromised. RCDP patients exhibit rhizomelic limb shortening, short stature, cataracts, mental retardation, epiphyseal and extra-epiphyseal punctate calcifications [42], degeneration of chondrocytes from resting cartilage [41] and defects on endochondral ossification [35]. As referred previously, plasmalogens are a major component of myelin and consequently abundant in the nervous tissue. Thus, it is expectable that peroxisomal disorders such as RCDP in which the plasmalogen biosynthesis is impaired or even blocked, develop myelin deficiencies. This was confirmed in experiments using cells from RCDP patients [43] where through magnetic resonance imaging (MRI) it was observed that these patients demonstrated abnormal white matter signal representative of dysmyelination, designating to

RCDP pathological abnormalities in the myelination process in form of demyelination, dysmyelination or reduction of myelin volume [44].

RCDP is a genetically heterogeneous disorder and is classified in three types that, although clinically indistinguishable, are divided according to defects in different genes [45].

RCDP type 1 is the most common of the three disorders [46]. It is characterized by mutations in the *PEX7* gene. The corresponding protein, Peroxin 7 (Pex7) belongs to the group of peroxisomal proteins and consists in a cytosolic receptor protein that recognizes proteins with the peroxisomal targeting signal 2 (PTS2) and targets them to the peroxisome. With Pex7 inactivated, proteins carrying PTS2 fail in being imported to the peroxisome [46], [47] and remain in the cytosol. There are three proteins described as having PTS2. 3-oxoacyl-CoA thiolase (ACAA1) is a peroxisomal enzyme responsible for the β -oxidation of very long chain fatty acids (VLCFAs) [48]. In RCDP patients this enzyme was described as being present in the cytosol of fibroblasts and liver cells in its precursor, non-cleaved and inactive form [49]. However, these patients did not exhibit VLCFA accumulation, indicating that the residual β -oxidation was sufficient to avoid *in vivo* VLCFA accumulation [49]. Furthermore, a diet dependent accumulation of phytanic acid is observed in RCDP patients due to the impaired action of phytanoyl-CoA hydroxylase (PhyH) [41] which is also a PTS2 carrying protein. Finally, Agps, which is also a PTS2 carrying protein [50], is mistargeted in RCDP type 1 patients resulting in a deficiency in the biosynthesis of plasmalogens [51].

RCDP type 2 presents a defect in a single peroxisomal enzyme due to mutations in the gene that encodes the first enzyme in the plasmalogens biosynthetic pathway - Gnpat - leading to a single defect in plasmalogen synthesis [52].

RCDP type 3 exhibits mutated forms of the gene that encodes the enzyme that performs the second step in the plasmalogen biosynthetic pathway - Agps - leading also to a single defect in plasmalogens biosynthesis [53], [54].

Despite having different genetic causes, comparisons of clinical presentations and pathology among these three variants of RCDP showed little differences, indicating that the defects observed may be mainly due to the deficiency in plasmalogens.

Some other human degenerative diseases have also been referred as having altered plasmalogen levels although they are not peroxisomal disorders.

There is still not a full knowledge about the importance of these changes, raising the question if the plasmalogen metabolizing products contribute to the pathology or if the decreased levels of plasmalogens are due to pathology associated conditions [2].

ALZHEIMER'S DISEASE (AD)

AD is a neurodegenerative disease and the most common form of dementia. It was shown in post-mortem brains from AD patients that the plasmalogen levels were decreased [55]. Several hypotheses have been put forward to explain the decrease of these ether phospholipids. On one hand, plasmalogens act as antioxidants and the high oxidative environment in AD increases the propensity of the vinyl-ether bond of plasmalogens to oxidative attack decreasing their physiological concentration. On the other hand, activation of psPLA2 may also contribute to the reduction of plasmalogen levels [24]. In addition, the described peroxisomal defect in AD may also cause plasmalogen defects [56] through its biosynthesis impairment. Despite all the factors, one cannot say if plasmalogen deficiency is a cause or a consequence in AD.

NIEMANN PICK TYPE C DISEASE (NPC)

NPC is a lysosomal storage disease characterized by an accumulation of unesterified cholesterol, glycosphingolipids and sphingomyelin with central nervous system (CNS) neurodegeneration [57]. It is caused by mutations in the genes NPC1 and NPC2 that are thought to be involved in the transport of cholesterol from endosomes to several intracellular destinations [5]. Experiments done with NPC mouse models demonstrated impairments in peroxisomal activities and decreased plasmalogen levels before the onset of the disease indicating that these events play a role in the initiation of the disease [58].

Other human disorders have been described as having plasmalogen levels decreased such as Down Syndrome, Neuronal Ceroid Lipofuscinosis which is an inherited neurodegenerative disorder with lipopigments accumulation in the lysosomal compartment, and Retinitis Pigmentosa, a X-linked and dominant and recessive autosomal disorder characterized by photoreceptor degeneration [3].

Plasmalogens form, thus, a strict relationship with several diseases, not only the ones related directly with its biosynthesis but also with others, such as neurodegenerative and metabolic disorders. This suggests an involvement of plasmalogens in the pathology of these diseases.

PLASMALOGEN DEFICIENT MICE MODELS

In order to evaluate the biochemical and phenotypic consequences of plasmalogen deficiency, different mouse models have been created to mimic the human disorders that are originated from this ether-phospholipid deficient synthesis. Currently, four different mouse models with defects in ether-phospholipids are available, *i.e.*, the Pex7 KO mouse [35], the Pex7 hypomorphic mouse [59], the Gnpat KO [34] and the Agps hypomorphic mouse [60]. In this work two of these four mouse models were used: Pex7 KO and Gnpat KO mouse model.

PEX7 KNOCKOUT MOUSE MODEL

The Pex7 KO mouse model was generated by Brites *et al.* [35] by deleting the exon 3 of the *Pex7* gene using homologous recombination and is used to mimic RCDP type 1. The deletion of *Pex7* gene does not cause embryonic lethality. This way, Pex7 KO mice are born alive. However, they present a mortality rate of approximately 50% in the first 24h which may be explained by some of the phenotypic features of this mouse model such as hypotonia and decreased mobility which would hamper the feeding process. Animals that subsist this critical period after birth, survive to adulthood being able to reach 18 months of age.

As physical aspects, these mice exhibit dwarfism and phenotypically they also present testicular atrophy, eye cataracts and infertility [35]. Biochemically, in the Pex7 knockout mouse model all proteins containing PTS2 fail in being imported to the peroxisome. ADHAP-S, the enzyme catalysing the second step in the plasmalogen biosynthetic pathway is an example of PTS2 carrying protein and when trapped in the cytosol suffers proteolytic degradation [5]. This way, the

plasmalogen biosynthetic pathway is impaired in Pex7 KO mice. Moreover, these mice exhibit a defective peroxisomal fatty acid β -oxidation and increased levels of VLCFAs in newborn pups that are normalized in adulthood. The α -oxidation is also impaired due to a mislocalization of PhyH [35].

Pex7 KO mice reveal also a deficiency in neuronal migration demonstrated by studies performed in the developing brain at E18.5 where the density of neurons in the intermediate zone of the neocortex was increased. Another physiological defect presented by Pex7 KO mice is the endochondral ossification process. Newborn pups exhibit an incomplete skull ossification and defects in the ossification of several cartilage based structures, hindlimbs and middle phalanges [35].

GNPAT KNOCKOUT MOUSE MODEL

The Gnpat KO mouse model was generated by Rodemer *et al.* [34] by deleting exon 5 to 7 of the *GNPAT* gene using homologous recombination and is used to mimic RCDP type 2. In Gnpat KO mice, there was described some embryonic lethality and a decreased lifespan (about 40% died within the first 6 weeks of age). Similarly with Pex7 KO mice, Gnpat KO animals that subsist the period after birth, survive to adulthood and reach also the 18 months of age. Interestingly, in this animal model, the majority of the long lived animals were females, indicating a disproportional death rate between genders [34].

Physically, Gnpat KO mice present dwarfism, shortening of the proximal limbs and are underweight. Moreover, male Gnpat KO mice are infertile in which adult testes are atrophic and spermatozoa are absent in the epididymis. Fertility problems exist also in female Gnpat KO mice. Physiologically, these animals exhibit also ocular abnormalities, namely cataracts and abnormal myelination in the optic nerve[34]. Biochemically, this mouse model does not produce Gnpat protein and consequently there is no measurable activity of this enzyme despite normal activities of Agps [34].

This way, the single enzyme mutation leading to a single plasmalogen deficiency may be an advantage for a more straightforward understanding between the biochemistry-pathology relationship.

PERIPHERAL NERVOUS SYSTEM MYELIN SYNTHESIS AND STRUCTURE

Glial cells and neurons are in a continuous and highly regulated bidirectional dialog. The myelination process is one example of this intercommunication where, in the central nervous system (CNS) the oligodendrocytes, and in the peripheral nervous system (PNS) the Schwann cells (SCs) are responsible for communicating with axons and proceed with myelin synthesis and maintenance [61].

Several neurological disorders such as leukodystrophies and peripheral neuropathies are a reflection of an impairment in the myelination process or of myelin degeneration.

One should keep in mind that, regarding its biochemical composition, myelin contains a very high lipid-protein ratio in which 70-80% of the myelin composition consists in lipids and 20-30% is protein. Amongst others, this characteristic provides myelin its insulating property necessary for the saltatory propagation of nervous impulse [62].

SCHWANN CELL AND PNS MYELIN SYNTHESIS

Schwann cells are derived from the neural crest [63]. At a very initial stage they derive from neural crest cells and evolve to a first intermediate stage in the SCs development process – the Schwann cell precursor – that is found in mouse at the embryonic day E12 and E13 (Figure 4). The second intermediate – Immature Schwann cell – is a product of evolution from the SC precursor stage and appears at E15 till the time of birth. Finally, around birth, and at the end of the development process, immature SCs start to generate the first myelinating SCs and subsequently the non-myelinating SCs. This way, SCs appear in the mature PNS as two different types of cells: the myelinating SCs which surround large axons and the non-myelinating SCs which engage smaller axons [64], [65], forming the Remak bundle.

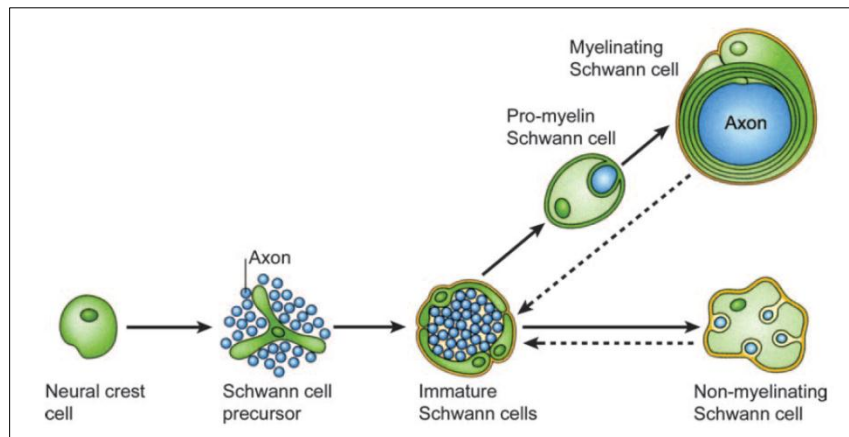


Figure 4. The Schwann cell development process in mouse, schematic illustration of the main cell types and developmental transitions in Schwann cell. There are three major transient cell populations in the Schwann cell lineage in the embryonic phase. The neural crest cells that originate the second cell population – Schwann cell precursors – and the third cell population, the immature Schwann cell that is the one that precedes the transition where myelinating or non-myelinating Schwann cells are formed. SCs that engulf large-diameter axons will be stimulated to myelinate and SCs that ensheath small-diameter axons evolve to mature non-myelinating Schwann cells. Note the reversible characteristic in the Schwann cell myelinating or non-myelinating stage demarcated by stippled arrows, which in part is responsible for the amazing ability of the PNS to regenerate. From [64], [65].

In the immature peripheral nerve, SCs engulf a large bundle of naked axons with varying diameters. The establishment of contact with these axons and the release of signals from the axons leads to SC proliferation [66]. These signals from axons regulate also survival and differentiation of Schwann cells and are also involved in the determination of myelin thickness [67], [68]. As the SCs proliferate, they start to direct their processes deeper into the axon bundle starting a segregation process, known as radial sorting, which eventually leads to a one-to-one relationship between a SC and a axon segment to be myelinated [69]. Simultaneously, a basal lamina starts to be secreted by the SC at the abaxonal (outer) surface of the Schwann cell/axon unit. This basal lamina formation is intricately related with the myelination process since it is thought to be one of the events that leads to the SC differentiation towards myelination [62], [70], [71].

As mentioned above, axons have the capability to release certain types of signals that stimulate the SC to differentiate and myelinate. However, only axons with a minimum diameter size are able to secrete those signals. So, Schwann cells will only be able to form a myelin sheath if they become in contact with axons with a diameter greater than $0.7\mu\text{m}$ [62]. After the occurrence of this

communication, SCs are able to wrap their plasma membrane around axons and, this way, generate multiple layers of myelin and ultimately myelinate nerve fibres capable of producing the rapid saltatory impulse conduction of the nervous system. On the other hand, Schwann cells in contact with small-calibre axons will become non-myelinating Schwann cells, engulfing several axons and giving rise to the so called Remak bundles [72].

The presence of axons is not only required for the expression of the myelin genes during development but also for the maintenance of the myelinating phenotype since injury and loss of axonal contact leads to downregulation of myelin gene expression [62], SC dedifferentiation and myelin breakdown [73] as part of a process called Wallerian degeneration. However, SCs have a remarkable characteristic of reversibility between their non-myelinating and myelinating stages (Figure 4). For example, after injury and SC dedifferentiation, the phenotype of these SCs becomes very similar to the phenotype of immature SCs that precedes myelination leading to a favourable environment for axon regrowth. After contacting with these regrowing axons, SCs proceed to redifferentiation and myelination, performing the so called process of nerve regeneration [65], [74].

PNS AXONAL AND SCHWANN CELL STRUCTURE AND COMPOSITION

The myelinated fibers have a well-defined structure and can be divided into four structural regions according to their typical molecular distribution and protein expression: the Internode, the Juxtaparanode, the Paranode and the Node of Ranvier (Figure 5 B).

The myelin sheath formed by the SC in the PNS enwraps the axon in segments that are separated by Nodes of Ranvier (Figure 5 A). These structures described as short, periodical interruptions in the myelin sheath are in the peripheral nerves covered by microvilli extensions of the Schwann cell (Figure 5 B) [67]. Regarding the regional expression of proteins, the node of Ranvier is characterized by a high abundance in Na⁺ channels essential in the action potential generation [75]. Other proteins particularly rich at the node are Ankyrin G [76] and the actin binding protein β IV Spectrin (Figure 5 C) [77].

Adjacent to the node is a specialized region called paranode which is a non-compact myelin region characterized by the presence of a complex of two

cell-recognition molecules – contactin associated protein (Caspr) and contactin that are involved in the axo-glial junctions and play important roles in cell adhesion and intercellular communication [78]. Together with the paranode, the Schmidt Lanterman incisures (SLI) consist in the only regions of non-compact myelin in the myelinated axon.

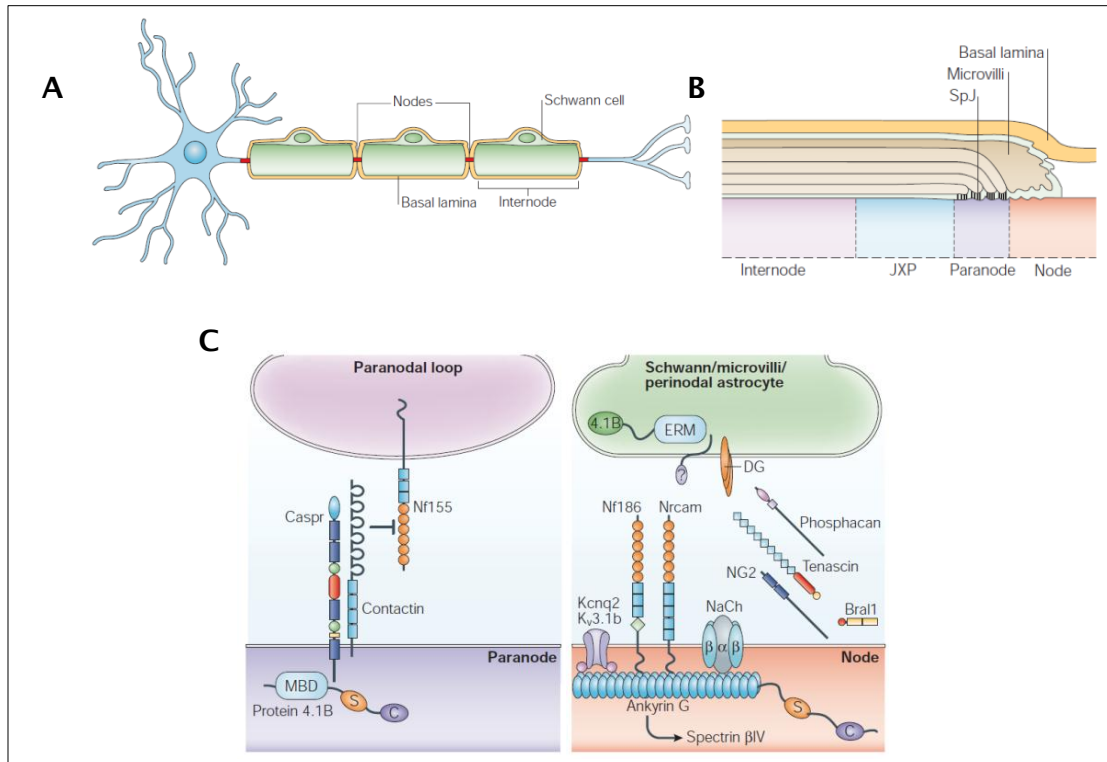


Figure 5. Structure of a PNS myelinated axon and the molecular composition in the different nodal regions. (A) Schwann cells in the PNS are responsible for myelination and enwrap several times the axonal segment forming the myelin sheath. Myelin covers the axon in defined segments forming the internode and leaving gaps – the nodes. (B) Longitudinal scheme of a myelinated fibre showing the different axonal regions. (C) Distinct expression of different molecules in the node and paranode. Na⁺ channels, AnkyrinG and βIV Spectrin are typically nodal proteins. Caspr and Contactin are present in the paranodal region. Figure adapted from [67].

The Schwann cell is also characterized by a specific cytoarchitecture where it presents a highly polarized configuration, both radially and longitudinally, necessary for the propagation of action potential [79]. A specific complex of proteins, namely the dystroglycan-dystrophin complex, is necessary for the correct function of SCs in the myelination process, including the determination of

the number of wraps that the SC performs around the axon and in the determination of the internodal length [80].

In the PNS, dystroglycan is present in the abaxonal membrane of the SC and whereas α -dystroglycan binds extracellular ligands such as laminin [81] and is anchored to β -dystroglycan, this latter one is a transmembrane protein in which its cytoplasmic tail interacts with cytoskeletal proteins namely f-actin [82].

The abaxonal Schwann cell membrane is compartmentalized into two distinct domains: the membrane covering the Cajal bands and the membrane directly apposed to the myelin sheath forming the appositions (Figure 6). Structurally, they differ in the way that in Cajal band compartment β -dystroglycan is cleaved in its extracellular tail by a metalloproteinase and forms a complex with Utrophin and Actin, while in the apposition compartment, β -dystroglycan forms an intracellular complex with Periaxin and DRP2 (Dystrophin related protein) and binds extracellularly to α -dystroglycan (Figure 6) [83].

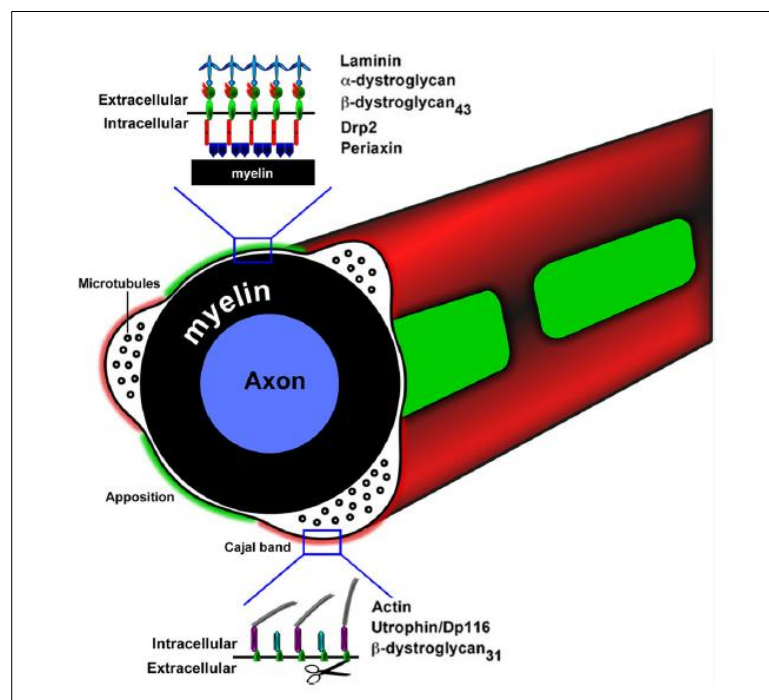


Figure 6. Schematic representation of the Schwann cell membrane compartments. Two different compartments are formed in the abaxonal SC membrane: the apposition that is composed by a complex formed by α -dystroglycan bound to non-cleaved β -dystroglycan, DRP2 and Periaxin. On the other hand, the Cajal bands are composed of a complex formed by α -dystroglycan bound to cleaved β -dystroglycan, Utrophin or Dp116 and Actin allowing cytoskeletal organization. The scissors illustrate the metalloproteases action. Figure adapted from [84].

REGULATION OF PNS MYELINATION – MOLECULAR MECHANISMS

Myelination process in the PNS is a highly regulated process that involves a bidirectional dialog between glial cells and neurons. This intercommunication is essential for myelin formation during development, myelin maintenance and also myelin regeneration after injury. While this axon-glia dialogue takes part, a healthy and functional nervous system is maintained [85].

Differentiation of neural crest cells to myelinating SCs requires the involvement of neuregulin-1 type III (NRG1-III), a key regulator involved in almost all aspects of the Schwann cell biology. NRG1-III produced by neurons in the CNS and PNS acts as a ligand that signals via tyrosine kinase receptors (ErbB2/ErbB3 heterodimers) present in the SC membrane [86]. The release of NRG1 from the axon is the factor that determines myelin thickness and is proposed to be the responsible element for the fact that axons $<1\mu\text{M}$ are not myelinated due to an insufficient amount of signalling molecule that is released. Myelin thickness is, this way, proportional to the axon diameter [87].

According to Pereira *et al.* [88], there are three major signalling pathways involved in the PNS myelination process activated by NRG1-III.

One of the major pathways corresponds to the PI3K/PIP3/AKT/GSK3 β signalling pathway [89]. Activation of this pathway by phosphorylation and activation of AKT leads to an activation of myelination. PTEN has an opposing effect over myelination through this pathway and inactivation of AKT experiments have shown to lead to hypomyelination [90].

The second major pathway involves increase of intracellular Ca^{2+} by Phospholipase C- γ (PLC- γ) activation. This process leads to dephosphorylation and nuclear translocation of NFATc4 which will form a complex with Sox10 and activate the transcription of Krox20 and P0 pro-myelination genes [91]. Finally, the third pathway is the MEK pathway where the latter one phosphorylates Yy1. Yy1 will induce Krox20 which in its turn will induce myelination [92].

The SC myelination is under a very strict transcriptional control [93] (Figure 7) which involves positive and negative transcription regulators. As examples of positive myelination regulators, there are Sox10 and Oct6 which have a synergistic effect in inducing the expression of Krox20. On the other hand, as negative myelination regulators, there are Sox2, c-Jun and Notch. Injury,

demyelination or disease lead to a dominant expression of negative transcription regulators of myelination [88].

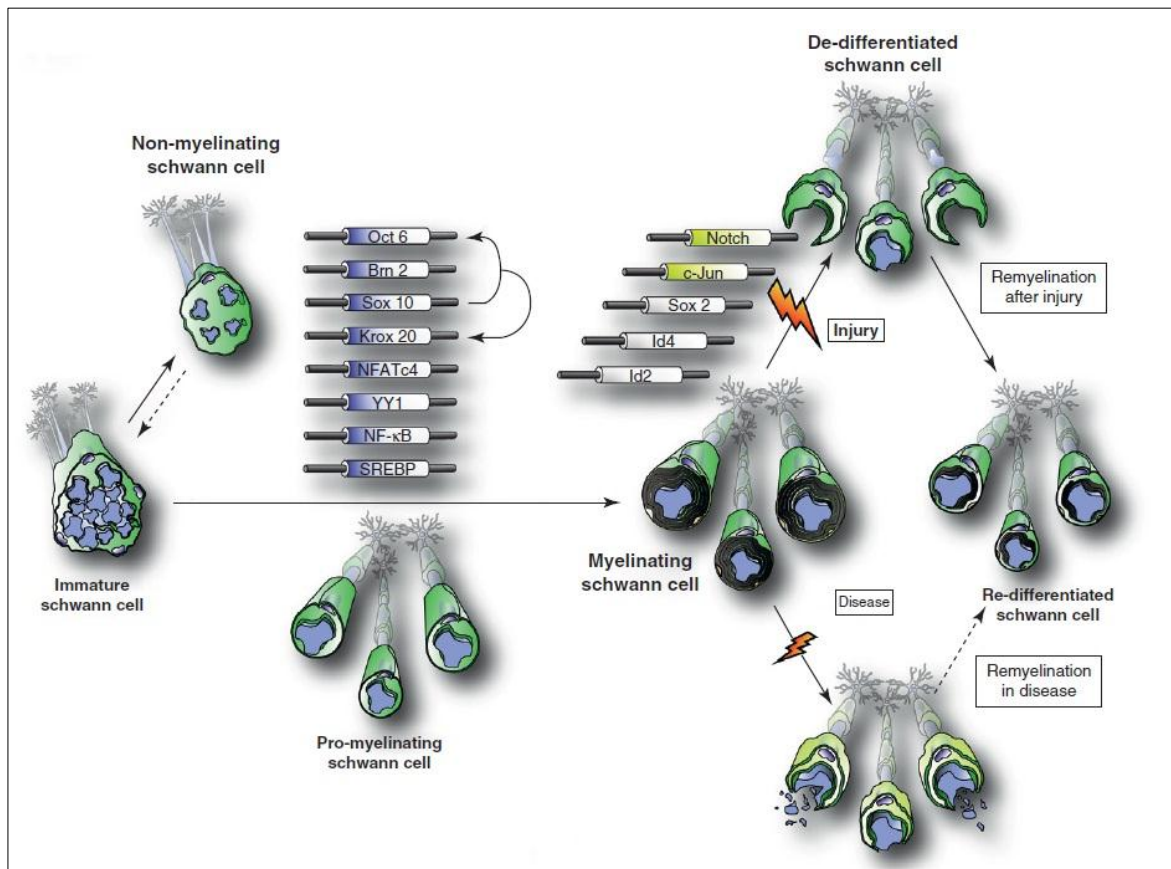


Figure 7. Transcriptional regulation of myelination in the PNS. During embryonic development SCs evolve until reaching the immature SC stage in which they are organized in SC-axon families where they surround axon bundles. Next, SCs perform radial sorting surrounding single axons $>1\mu\text{m}$ of diameter reaching a one-to-one SC-axon relationship achieving the pro-myelinating SC stage. SCs that do not engulf single axons acquire a non-myelinating state in which they surround multiple small calibre axons forming the Remak bundles. The main positive transcription regulators of myelination are represented in blue and the most important transcription regulators are Sox10 which activates Oct6 and that together will induce Krox20. The latter one is the main regulator of the ensuing myelination program. The main negative transcription regulators of myelination are represented in white and yellow. They are typically under regulation of the positive regulators, however, upon nerve injury the negative regulators dominate and direct SC demyelination. Notch, c-Jun and Sox2 are the most important negative myelination regulators. Figure adapted from [88].

PLASMALOGENS IN NERVOUS TISSUE

Given the enrichment of plasmalogens in the nervous tissue, it has been proposed that they have an important role in the normal function of neurons and myelinating glia. In fact, several studies involving cell lines of oligodendrocytes have described an enrichment of peroxisomes in these cells, associated to the necessity of lipid synthesis for myelin sheath assembly. Impairments in peroxisome assembly or function lead to myelin sheath degeneration and axonal loss [94][95]. In addition, the observation that several leukodystrophies and neurodegenerative diseases are characterized by defects in plasmalogens reinforces their importance for the normal function of the nervous tissue. In fact, studies performed in order to clarify the relationship between AD and plasmalogen have demonstrated that with the progression of the disease, the plasmalogen levels decrease [55]. There is still not sufficient evidence of whether the decreased levels of plasmalogens are a cause or a consequence of the disease, however, recent suggestions have been made relating the AD pathology to an inactivation Agps [96]. In AD pathological conditions the increase in ROS and A β peptide impairs the peroxisomal functions leading to a deficient import of Agps and plasmalogen biosynthesis blockade. Moreover, due to the elevated ROS values and due to the susceptibility of the vinyl ether bond in plasmalogens to suffer oxidation, plasmalogens levels in AD decrease [96].

In RCDP patients, the primary defect in plasmalogens causes both neuronal and myelination defects. As such, the understanding and elucidation of the pathologies, mechanisms and players of the disease, is crucial for RCDP and the larger group of neurological disorders, which contain a secondary defect in plasmalogens, which may worsen the disease state and/or pathology.

C

CHAPTER II

AIMS OF THE THESIS

The myelin sheath is of an extreme importance in biological organisms and plays innumerable crucial roles for the normal function of the nervous system. Among all of its functions, myelin is indispensable for a rapid conduction of the nervous impulse and functions also as a protective agent for the axon. The importance of the myelination process is highlighted by the presence of several pathological conditions derived by a progressive degeneration of the myelin sheath.

The main aims of this Master thesis were the determination of the importance of plasmalogens for the myelination process and the characterization of myelin's structure and composition. In addition, we aimed at determining and characterizing the molecular mechanisms behind the severe pathology. Finally, an equally important goal of this work was the development of a therapeutic approach which would reveal itself effective in the prevention or improvement of the neuropathological consequences of a deficiency in plasmalogens.

C

CHAPTER III

MATERIALS AND METHODS

ANIMAL HANDLING AND MOUSE MODELS

Mice were housed under specific pathogen-free conditions and all animal experiments were performed according to the guidelines of the Portuguese National Authority for Animal Health (DGV), the European Union directive 2010/63/EU and according to the institutional rules. Animals were handled and experiments were performed by FELASA-accredited researchers.

PEX7 AND GNPAT KNOCKOUT MICE MODELS

The *Pex7* and *Gnpat* knockout mice used in all experiments were maintained on a Swiss-Webster background and obtained crossing heterozygous *Pex7* or *Gnpat* breeding pairs. Wild-types (WT) are littermates from *Pex7* and *Gnpat* knockout mice. Mice were maintained at $24\pm 1^\circ\text{C}$, at a 12h dark/light cycle and fed *ad libitum*.

Mouse genotyping was performed using genomic DNA extracted from ear clipping in the IBMC CCGen facility following the strategies previously developed [45], [97].

LICL TREATMENT

For the lithium chloride (LiCl) treatment, mice were injected subcutaneously with 50mg/kg of LiCl using a 30G needle. Two different setups (A and B) were performed according to the scheme of Figure 8. For the control condition, mice were injected with sodium chloride (NaCl) 50mg/kg. After treatment, mice were euthanized by decapitation and sciatic nerves as well as leg muscles were collected and frozen for further analysis (see below *biochemical assessment*). Furthermore, sciatic nerves were also collected and fixed for histological assessment as described below in *Histological assessment of sciatic nerves*.

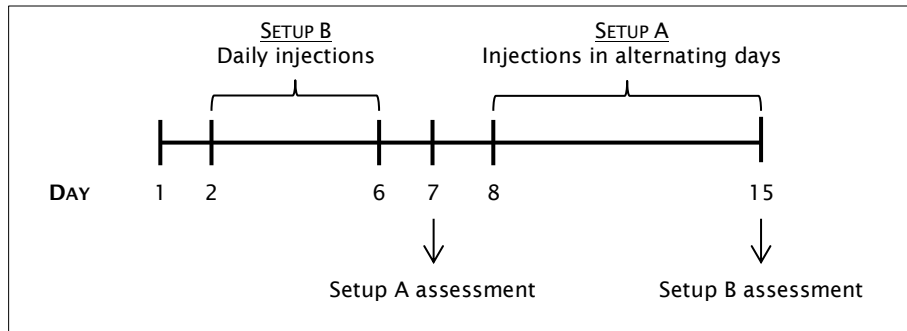


Figure 8. Representative scheme describing the LiCl treatment strategy. Setup A consists in an every second day treatment from P7 to P15. At that day, Setup A LiCl treated mice were euthanized and tissues were collected for further analysis. Setup B consists in a daily treatment from P1 to P6. At P6, Setup B LiCl treated mice were euthanized and tissues were collected for further analysis. Control animals treated with NaCl were subjected to the same setups.

HISTOLOGICAL ASSESSMENT OF SCIATIC NERVES

SCIATIC NERVE FIXATION AND PROCESSING

Previously isolated sciatic nerves from 17 months old Pex7 knockout mice and correspondent WT littermates, as well as from LiCl and NaCl treated Gnat knockout mice and correspondent WT littermates were processed for histological analysis.

Sciatic nerves were fixed in glutaraldehyde (GTA) (4% of GTA in 0,1M of sodium cacodylate), post-fixed in osmium tetroxide and embedded in epon for further processing to semi-thin and ultra-thin cross sections. Semi-thin cross sections of 1 μ m were stained with p-phenylenediamine (PPD) for g-ratio analysis and/or fibre density calculations. Ultra-thin cross-sections of 50nm of thickness were stained with uranyl acetate and lead citrate for electron microscopy (EM) analysis.

MORPHOMETRIC ASSESSMENT OF SCIATIC NERVE FROM 17 MONTHS OLD MICE

Using Photoshop software and 40x montage pictures of sciatic nerves from semi-thin cross-sections, fibre density was calculated counting all fibres in the nerve and dividing it by the nerve area. G-ratio evaluation was performed calculating the ratio between the axon diameter and the fibre diameter (includes the myelin sheath) and over 200 fibres in each cross-section of every animal were

analysed. Ultra-thin cross sections were assessed taking photographs at 8000x magnification in the transmission electron microscope (TEM Jeol JEM-1400) equipped with an Orius SC1000 Digital Camera.

MORPHOMETRIC ASSESSMENT OF SCIATIC NERVE FROM LiCl TREATED MICE

Ultra-thin cross sections were analysed taking photographs at 5000x magnification in the transmission electron microscope (TEM Jeol JEM-1400) equipped with an Orius SC1000 Digital Camera.

TEASED FIBERS

For the teased fibers experiments, the method of Court *et al.* [80] was followed. Mice were anesthetized with ketamine and medetomidine (100mg/kg and 1mg/kg respectively), euthanized and exsanguinated. Sciatic nerves were isolated and fixed with 4% Paraformaldehyde (PFA) in PBS. Under the dissection microscope and using 38G needles, the nerve was separated in several bundles (~0,5cm in length and as thin as possible). The bundles were blocked for 1hr at room temperature (RT) with 10% Normal Donkey Serum (NDS) and permeabilized with 10% NDS + 0.1% Triton. Immunofluorescence assay was done with primary antibody (see Table 2) over-night (O/N) at 4°C and Alexa fluor secondary antibody for 2 hours at RT. The bundles were teased into single fibers in the silane-treated slides within a drop of Vectashield+DAPI. Afterwards, the slides were observed under the Epifluorescence microscope (AxioImager Z1 - Carl Zeiss Germany) and images of 20x and 63x magnification were taken in order to assess structural aspects of the fibers. Evaluation on the confocal microscope (Laser Scanning confocal microscope Leica TCS SP5 II) was also performed with 63x magnification pictures.

IN VITRO MYELINATION ASSAY

Dorsal root ganglia (DRG) were collected from E13.5 (embryonic day 13.5) embryos and digested in 0.25% Trypsin-EDTA. Cells were plated in matrigel coated cover slides at a density of 6 DRGs per well and maintained at 37°C. The

plating medium consists in DMEM high glucose with 2mM of L-glutamine, 10% FBS (Fetal bovine serum), 50ng/ml of NGF (nerve growth factor) and 1% P/S (Penicillin/Streptomycin). On the second day of culture, cells are put in a growing medium with Neurobasal, L-glutamine, NGF, Glucose 4g/L and B27 (gibco) during 10 days. On the 11th day of culture, cells are put in a myelinating medium with DMEM high glucose, L-glutamine, FBS, NGF and 50µg/ml of Ascorbic acid (AA) (Sigma) during 11 days. The culture is stopped on the 22nd day of culture with fixation of cells with 4% PFA. Cells were permeabilized with 100% Methanol and blocked with 5% NDS for 1 hour at RT. Immunofluorescence assay was done with primary antibody (see Table 2) O/N at 4°C and Alexa fluor secondary antibody for 1 hour at RT (Figure 9).

IN VITRO MYELINATION ASSAY WITH LiCl TREATMENT

For the *in vitro* LiCl treatment, a normal DRG explant culture for *in vitro* myelination assessment was performed. The administration of LiCl at a concentration of 16mM started on the 7th day of culture and was always added on the days that the medium was changed. Together with LiCl, Forskolin at a concentration of 3µM was also added.

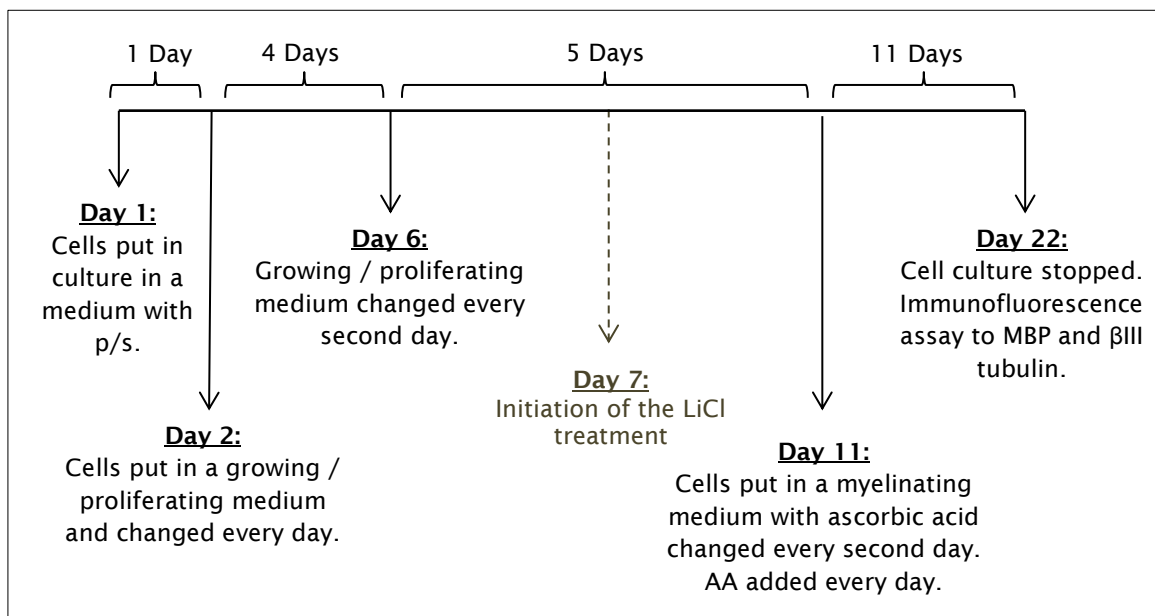


Figure 9. Representative scheme of the *in vitro* myelination assay. DRG co-cultures were maintained for 22 days and assayed for immunofluorescence with β III tubulin which stains neurites and MBP that marks myelinated segments. LiCl (or NaCl for controls) treatment is shown in grey with stippled arrows.

CELL CULTURE

MOUSE EMBRYONIC FIBROBLASTS (MEFs) CULTURE

Mouse embryonic fibroblasts were collected from embryonic day 12. After removing heart, liver and all dark tissues, the remaining carcass was minced and trypsinized (Gibco 25300) at 37°C for 10 min. Afterwards, single cell suspension was obtained by up and down using a 1000µl filter tip cut at the tip and posteriorly plated on T45 flasks with DMEM high Glucose, 10% FBS and 1% P/S.

FBS STIMULATION OF MEFs

Low passage number MEFs cultures in 3.5cm diameter culture dishes were allowed to grow until 80% confluence in a medium composed of DMEM high glucose, 10% FBS and 1% P/S. At this point, the cultures were subjected to serum starvation with medium containing 0.1% FBS for 12 hours. FBS induction was accomplished by adding medium containing 10% FBS and cells were incubated for 0, 1, 3 and 5 minutes. After the incubation period, medium was quickly removed, and cells were washed with ice-cold PBS. Three independent experiments were performed. Lysates were prepared by adding ice-cold lysis buffer (see below in *Biochemical Assessment* the protein extraction buffer). Cells were scrapped with rubber policemen and collected into an eppendorf and placed on ice for further biochemical assessment through Western Blot (see *Biochemical Assessment*).

BIOCHEMICAL ASSESSMENT

SAMPLE PREPARATION AND WESTERN BLOTTING

Using sciatic nerves, leg muscle samples or MEFs, protein extraction was performed using a lysis buffer (PBS plus 0.3% Triton, 1x Complete Mini Protease inhibitor (Roche) and 1mM sodium orthovanadate).

Using a glass holder vial with ice water, tissues were sonicated (3 pulses of 10 seconds, 35% cycle and 10% power) and centrifuged at 10000rpm for 5min at 4°C. Protein quantification was performed with the method of Lowry using a Bio-Rad protein assay kit (BioRad DC Protein Assay) and optical density was measured at 750nm.

Samples containing an equal amount of protein (25 µg) were run on 12.5% SDS PAGE gels and afterwards proteins were transferred to nitrocellulose membranes (Hybond™ ECL Amersham Biosciences).

Blots were blocked in 5% NFDM (non-fat dry milk) in Tris buffer saline (TBS) with 0.1% Tween for 1 hr at RT. Primary antibodies were diluted in 5% BSA (bovine serum albumin) in TBS with 0.1% Tween and incubated either for 1 hr at room temperature or O/N at 4°C depending on the antibody in question (see Table 2). Horseradish-Peroxidase conjugated Secondary antibodies were diluted in 5% NFDM in TBS with 0.1% Tween, used at a 1:5000 dilution and incubated for 1 hr at RT. Immunodetection was performed by chemiluminescence, using ECL system Western Blotting detection reagents (Pierce western blotting substrate) and membranes were exposed to Amersham Hyperfilm ECL (GE Healthcare) and the film was developed.

Blots were scanned either on a Molecular Imager GS800 calibrated densitometer (Bio-Rad) or on a Epson Perfection 4490 Photo scanner and quantified using Quantity One 1-D Analysis Software v 4.6 (Bio-Rad).

SUBCELLULAR FRACTIONATION

For the separation of different subcellular fractions, a Subcellular Proteome Extraction kit was used (539790 ProteoExtract® Subcellular Proteome Extraction kit – Millipore) that delivers four distinct protein fractions: fraction 1 (cytosolic fraction), fraction 2 (membrane/organelle protein fraction), fraction 3 (nucleic protein fraction) and fraction 4 (cytoskeletal fraction).

Low passage number MEFs cultures in 3.5cm diameter culture dishes were allowed to grow until 80% confluence in a medium composed by DMEM high glucose, 10% FBS and 1% P/S. At this point, the starvation protocol previously described in *FBS stimulation of MEFs* was performed at three different time-points: 0min, 3min and 5min. Subcellular fractionation protocol was performed according to the kit's datasheet and the entire protocol was executed with the cells in gentle agitation and at 4°C.

Initially, cells were washed twice for 5min with Wash Buffer. The cells were then incubated for 10min with Extraction Buffer I. The resulting supernatant (Fraction 1) which contains proteins extracted from the cytosolic fraction was

transferred to an eppendorf. The remaining cellular material was incubated with Extraction Buffer II for 30min and the corresponding supernatant (Fraction II) contains membrane/organelle proteins. Extraction Buffer III together with a nuclease solution was incubated for 10min and fraction III containing nuclear proteins was gathered to its correspondent eppendorf. The remaining cellular material was finally incubated with Extraction Buffer IV leading to obtainment of Fraction IV containing cytoskeletal and matrix proteins.

The different subcellular fractions were frozen for further biochemical assessment.

STATISTICAL ANALYSIS

For statistical analysis the graphpad software was used and results were expressed as the mean \pm s.e.m.. Comparison data between groups was performed using either Student's t-test, one way ANOVA with Tukey's post-test, or Mann Whitney test. $p < 0.05$ was considered statistically significant.

Table 2. Summarized list of antibodies used in this work. Includes information about the host, the purpose of the utilization of the antibody, its dilution and the supplier.

ANTIBODY	HOST	PURPOSE/DILUTION	SUPPLIER
DRP2	Rabbit	ICC / 1:300	Peter Brophy
Caspr	Rabbit	ICC / 1:2000	Elior Peles
β III Tubulin	Rabbit	ICC / 1:600	Epitomics
MBP	Rat	ICC / 1:250	Chemicon
p-AKT (Ser473)	Rabbit	WB / 1:1000	Cell Signalling
p-AKT (Thr308)	Rabbit	WB / 1:1000	Cell Signalling
T-AKT	Rabbit	WB / 1:1000	Cell Signalling
p-GSK3 β (Ser9)	Rabbit	WB / 1:1000	Cell Signalling
T-GSK3 β	Rabbit	WB / 1:1000	Cell Signalling
p-c-Raf	Rabbit	WB / 1:1000	Cell Signalling
Caveolin	Rabbit	WB / 1:5000	Transduction Laboratories
GAPDH	Rabbit	WB / 1:1000	Cell Signalling
ACAA1	Rabbit	WB / 1:1000	Sigma-Aldrich
Tubulin	Rabbit	WB / 1:1000	Cell Signalling
Sox 2	Rabbit	WB / 1:1000	Abcam
Oct 6	Rabbit	WB / 1:1000	Abcam

C

CHAPTER IV

RESULTS

Previous work at the Nerve Regeneration group has revealed that a plasmalogen deficiency affects the development and functioning of the peripheral nervous system (PNS) (Figure 10) [98]. Using Pex7 and Gnpat KO mice, it has been shown that a plasmalogen deficiency impairs: (i) the process of radial sorting, with a failure in the correct segregation of large calibre axons from axon bundles; (ii) myelination, as plasmalogen-deficient mice have increased g-ratio during the first 4 weeks of postnatal development of the PNS; and (iii) nerve conduction, with increased latencies of compound muscle action potentials. Given these observations, the aims of this Thesis were to elucidate the defects in myelination and myelin maintenance and unravel the mechanisms behind the neuropathy caused by a deficiency in plasmalogens.

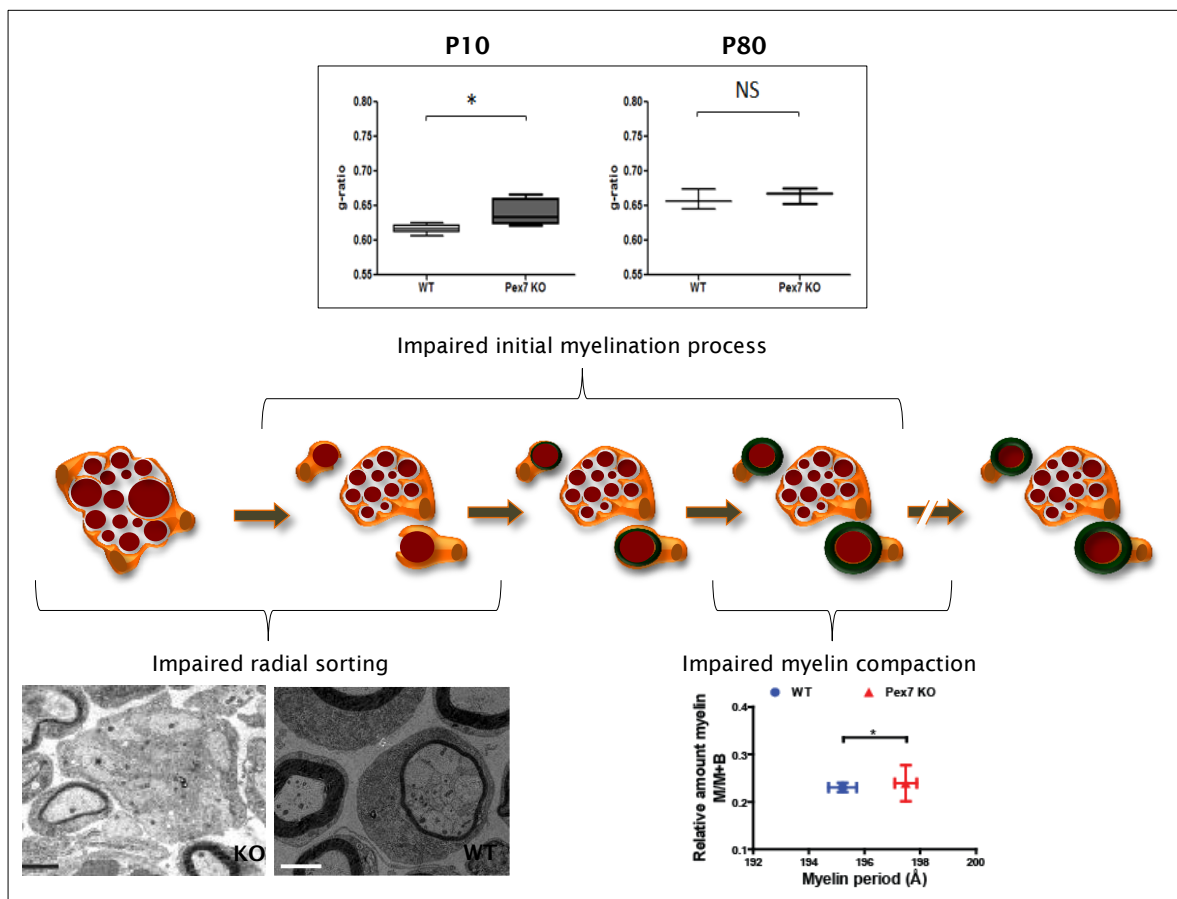


Figure 10. Consequences of plasmalogen deficiency to PNS. Plasmalogen deficient mouse models (Pex7 KO and Gnpat KO) have been used to assess the pathology caused by the absence of these ether-phospholipids. During the lifespan of mice, plasmalogens contribute to the myelination process in different ways and timepoints. On a very initial stage of the myelination process, a plasmalogen deficiency causes both impaired radial sorting (lower panel, left) and impaired myelination. However, in adult mice, the defect in myelination is rescued (upper panel), although x-ray diffraction analyses showed that myelin devoid of plasmalogens is less compact (lower panel, right).

DEMYELINATION IN THE ABSENCE OF PLASMALOGENS

As adult plasmalogen-deficient mice showed normal myelination we hypothesized that given the initial hypomyelination the formation and/or maintenance of myelin would be impaired.

The phenotypic characterization of Pex7 and Gnpat KO mice, supported our hypothesis, as mice older than 1 year acquired a progressive neuropathy with tremors and generalized ataxia, leading to hindlimb paralysis. We evaluated nerve pathology in Pex7 and Gnpat KO mice that reached the humane end point (around the age of 17 ± 1.9 months). Histological analysis of sciatic nerve sections stained with PPD showed that in comparison with WT nerves, nerves from Pex7 KO mice presented a pronounced demyelination and loss of myelinated fibers (Figure 11 A and B).

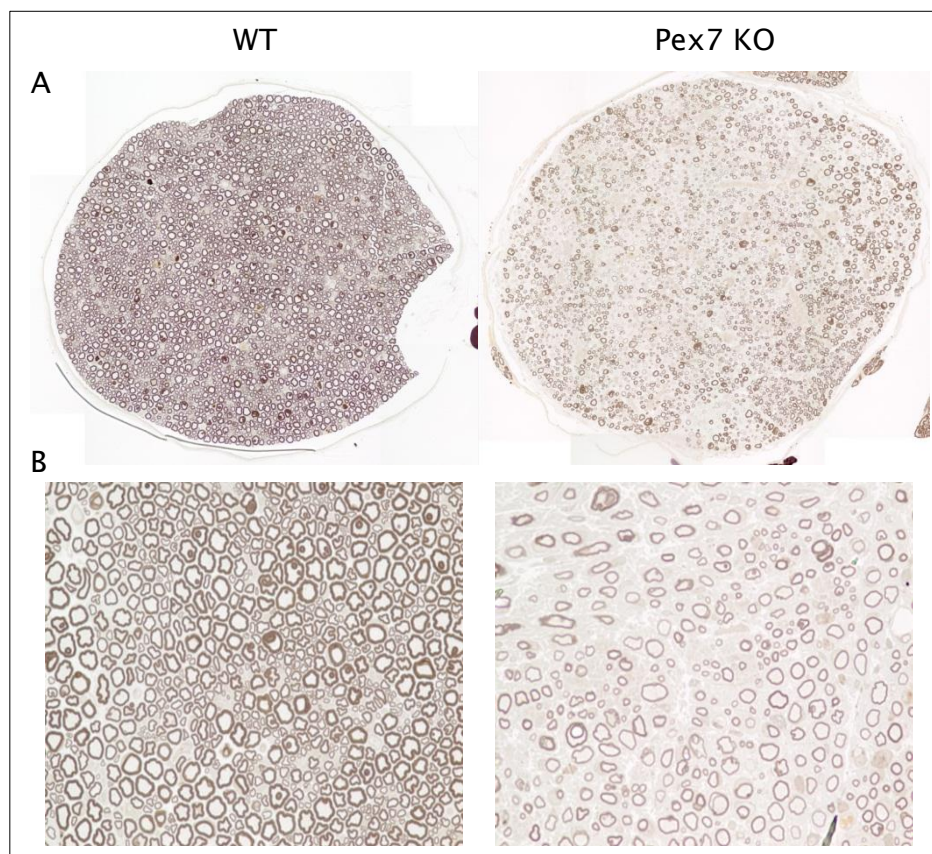


Figure 11. Deficiency in myelin maintenance in the absence of plasmalogens demonstrated by an age-dependent demyelination. Semi-thin cross-sections of sciatic nerves from 17 months old WT and Pex7 knockout mice were stained with PPD to enable the visualization of myelin. Panels in A correspond to 10x montage pictures and panels in B represent the corresponding sciatic nerve from the overhead panel at a 40x magnification. Nerves from Pex7 KO mice have a striking visible pathology comprised of loss of myelinated fibers and loss of myelin.

A similar pathology was observed in nerves from aged Gnpat KO mice (data not shown). Quantifications revealed a 2-fold decrease in the density of myelinated fibers in Pex7 KO nerves (Figure 12 A). The determination of the g-ratio, confirmed the demyelination status of nerves from KO mice but it also revealed that myelin loss was predominant in large-calibre axons, as axons with a diameter smaller than $3\mu\text{m}$ had normal g-ratio (Figure 12 B).

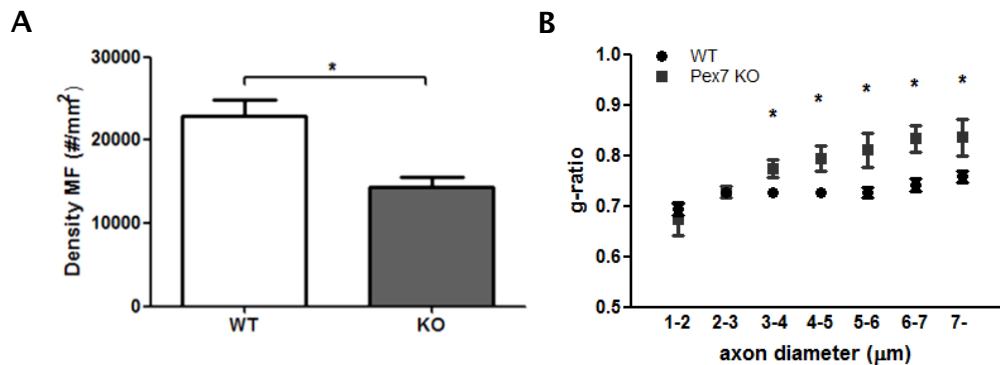


Figure 12. Absence of plasmalogens leads to axon loss and demyelination. The density of myelinated fibers decreases in aged Pex7 KO mice (A) and g-ratio values show that, in the absence of plasmalogens, with an increasing axon diameter, g-ratio increases (B). WT n=4 and KO n=5. For g-ratio evaluation over 200 MF were assessed. Statistical analysis was performed using Student's T-test. Error bars show s.e.m. and * = $p < 0.02$.

The results obtained with the histological analysis warranted a more detailed ultrastructural analysis, to unravel the extent of the demyelination and determine if the observed loss of myelinated fibers was due to complete lack of myelin as completely demyelinated axons are not stained with PPD or due to an actual loss of axons. The electron microscopic analysis, revealed a striking pathology in the nerves from aged Pex7 KO mice (Figure 13). Axonal loss was evident in mutant nerves, with reduced number of axons regardless of the myelination status. Nevertheless, the lack of plasmalogens had a profound effect in Schwann cells, as we observed completely demyelinated axons (left fibre with asterisk), severely demyelinating axons (right fibre with asterisk), and possibly remyelinating axons (middle fibre with asterisk). In mutant nerves, we observed signs of remyelination as small calibre axons had normal g-ratio (Figure 12) and the electron microscopy analysis also indicated that these small calibre axons contained normal myelin. In addition, we observed that the endoneurium of

mutant nerves is filled with Schwann cell processes (arrows). These processes seemed to represent failed attempts of Schwann cells to remyelinate demyelinated or demyelinating axons. The Schwann cells act to the demyelination by extending process to wrap axons in order to attempt remyelination. The failure in accomplishing this, coupled with the excessive production of the processes creates the appearance of structures similar to onion-blubs, which consist in the formation of redundant basal lamina and are the hallmark signs of failure in remyelination. Nevertheless, we also observed Schwann cell processes around unmyelinated axons in Remak bundles, suggesting that the mutant phenotype in Schwann cells from KO mice may also be unrelated to myelination.

Combined, our results demonstrate that the deficiency in plasmalogens severely affects Schwann cells and myelination. Given the extent of demyelination during aging and the evidences for failure in remyelination, we hypothesize that the axonal loss is secondary to the demyelination.

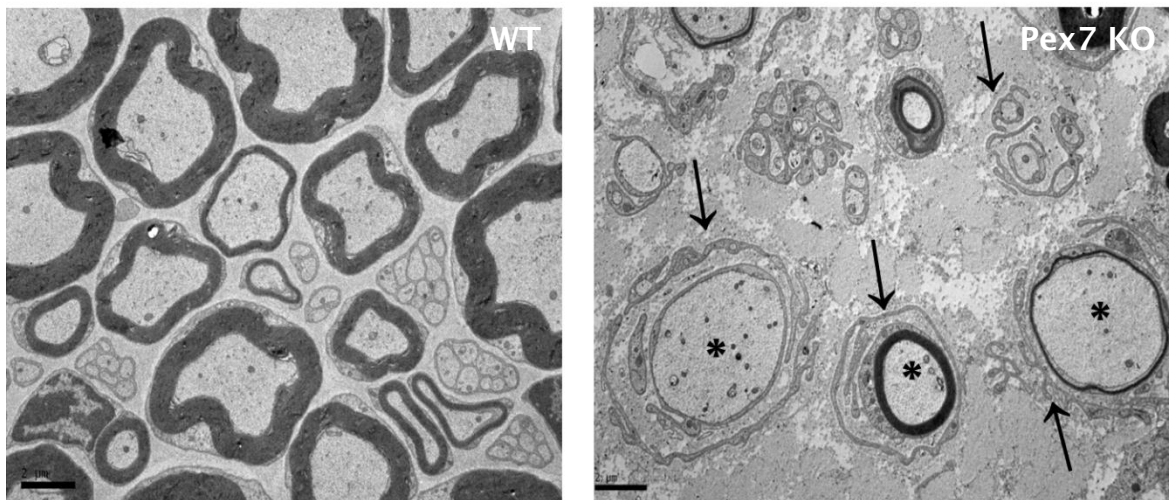


Figure 13. Sciatic nerves from plasmalogen deficient mice exhibit axon loss, demyelination and failure to remyelinate. Electron microscopy assessment of nerves from Pex7 KO mice showed clear signs of demyelination, with axons lacking (left asterisk) or containing considerable less myelin (right asterisk) and the formation of Schwann cell processes (arrows). Scale bar = 2 μ m.

DISORGANIZED MYELIN IN THE ABSENCE OF PLASMALOGENS

The preceding results, combined with the previous characterization of the myelination process presented in Figure 10, indicate that the functions and roles of Schwann cells are severely compromised in a plasmalogen deficiency. This way, we hypothesised that despite the observation of normal g-ratio in nerves from adult plasmalogen-deficient mice, the deficiency could affect the structure and organization of the myelinating Schwann cell.

In order to analyse the structure and organization of myelinated fibers, we performed immunofluorescence in teased fibers, to determine the pattern and levels of proteins that function as markers for distinct regions of a given myelinated fibre. Antibodies against Caspr were used to label the axonal paranode, antibodies against DRP2 were used to label the Schwann cell appositions, and Phalloidin, which labels f-actin, was used to stain non-compact myelin.

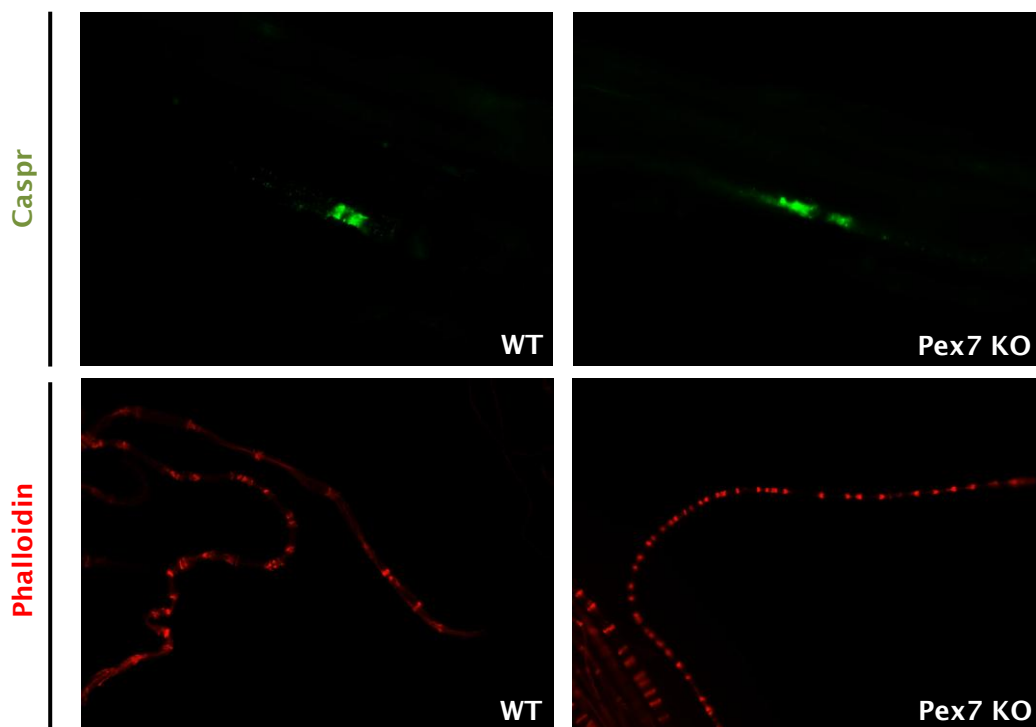


Figure 14. Myelin structure and composition is altered in the absence of Plasmalogens. Epifluorescence microscope images of Caspr and Phalloidin show that, compared with WT, adult Pex7 KO mice exhibit an altered paranode assembly demarked with Caspr and contain an increased number of Schmidt-Lanterman incisures demarked with Phalloidin. Upper panel pictures are at a 63x magnification and lower panel pictures are at a 20x magnification.

Caspr labelling in teased fibers from WT nerves, revealed the paranodal region (Figure 14, upper panel). However, we observed a less demarked paranodal region and a more diffused staining in teased fibers from Pex7 KO mice, suggesting a defective recruitment of Caspr to this axonal region due to a defective paranodal assembly. Phalloidin staining was performed in order to assess the cytoskeletal organization of the myelinating Schwann cells. By staining for f-actin we could visualize the Schmidt-Lanterman incisures, which are regions of non-compact myelin involved in metabolic processes of the myelin sheath and communication across the myelin sheets which are vital to myelin function [99][100][101]. Our analysis revealed an increase in the number of Schmidt-Lanterman incisures in teased fibers from Pex7 KO nerves (Figure 14, lower panel). Combined with the observations using X-ray diffraction that showed larger myelin periodicity in sciatic nerves from Pex7 KO mice (Figure 10) [98], our results indicate that, in general, plasmalogen-deficient myelin is less compact.

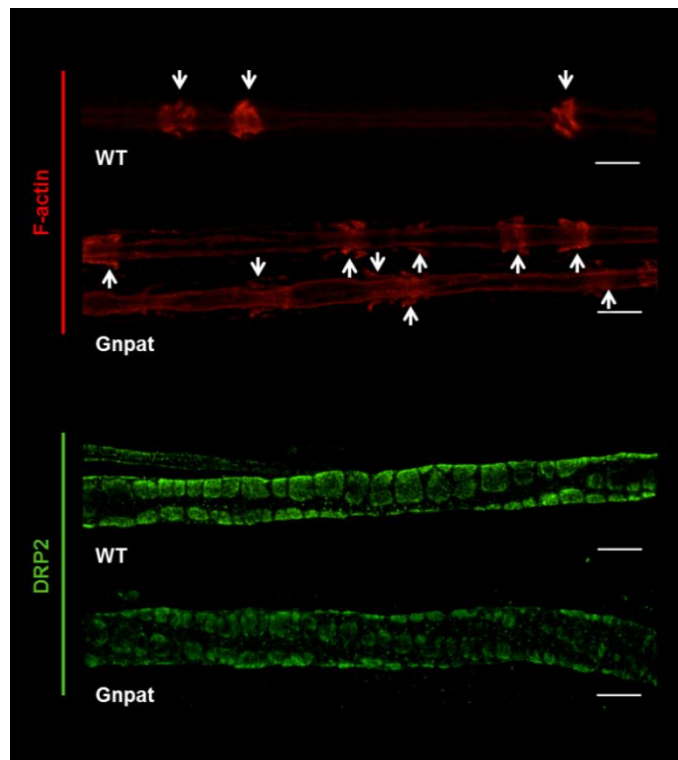


Figure 15. Plasmalogen deficiency leads to abnormal myelin in structure. Confocal analyses of f-actin and DRP2 in nerves from Gnpat KO mice demonstrated an increase in the number of SLI (upper panel) demarked with Phalloidin (f-actin) and an abnormal compartmentalization of the Schwann cell's plasma membrane (lower panel) demarked with DRP2. Scale bar is 10 μ m.

DRP2 immunolabeling was performed to assess the compartmentalization of the cytoplasm from Schwann cells. Our analysis revealed a fragmented and disorganized pattern of DRP2 labelling in Pex7 KO nerves indicative of a disorganization of the appositions and abnormal compartmentalization of the SC's plasma membrane. In order to corroborate that the abnormalities found in Pex7 KO nerves were solely due to the defects in plasmalogens, we also analysed teased fibers from Gnpat KO mice. For this, we used 9 months old mice as not to use mice within ongoing demyelination. Our analyses (Figure 15) using f-actin and DRP2 staining revealed that the lack of plasmalogens causes an increase in the number of Schmidt-Lanterman incisures and disorganized appositions.

Combined, our results showed that plasmalogen-deficient nerves are initially characterized by hypomyelination, and that despite reaching normal amounts of myelin (normal g-ratio), they are dysmyelinated and acquired a progressive and severe demyelination.

DEFECTIVE MYELINATION IN THE ABSENCE OF PLASMALOGENS

Given the complexity of the myelination process and the different defects observed in plasmalogen-deficient nerves, we performed *in vitro* myelination assays to assess the role of plasmalogens in myelination with another type of approach besides g-ratio determination, and without confounding effects including delays in development.

in vitro myelination assays were performed according to well described strategies [102], [103]. DRG co-cultures of neurons and Schwann cells from E13.5 embryos were maintained in culture for 22 days and stimulated to myelinate for the last 11 days by the addition of ascorbic acid. Immunofluorescence assays for β III tubulin allowed the evaluation of neurite growth, density and viability. When comparing WT with Gnpat KO co-cultures, there was no observable difference in neurites (Figure 16 A, left panel), as plasmalogen deficient DRG neurons are able to produce a normal grid of neurites. However, when assessing by immunofluorescence staining of myelin basic protein (MBP), which marks myelinated segments and allows the evaluation of the myelination status of the cultures, the results were quite different. Gnpat KO co-cultures exhibited a

notable impairment in the myelination process demonstrated by the MBP immunolabeling (Figure 16 A, right panel).

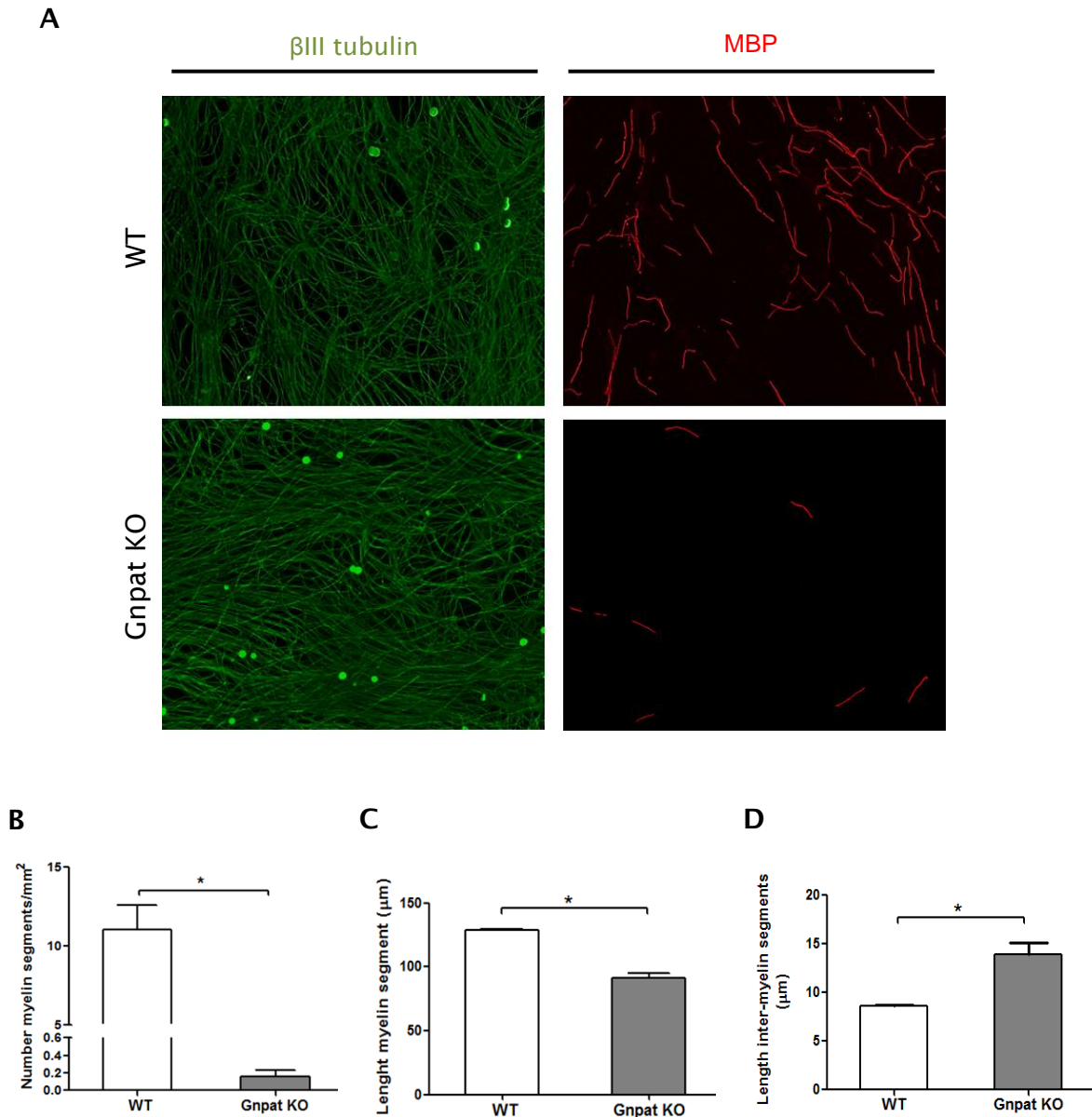


Figure 16. Defective *in vitro* myelination in the absence of plasmalogens. Results from *in vitro* myelination assays with DRG co-cultures from WT and Gnpat KO mice revealed no differences in the formation of a neurite network, as judged by immunolabeling with anti-tubulin- β III (green labelling in A). Assessment of myelination by MBP immunolabeling revealed fewer and shorter myelin segments in co-cultures from Gnpat KO mice (red labelling in A). Quantifications of density (B) and length (C) of myelin segments, confirmed the immunohistological analyses, with a decreased number and length of myelinated fibers. Quantification of the paranodal length (D) also showed that in Gnpat KO co-cultures the distance between two adjacent myelinated segments is increased. Statistical analysis was performed using Student's T-test. Error bars show s.e.m. and * = $p < 0.03$.

Further analysis was performed in order to obtain not only qualitative information but also a quantitative assessment of the degree of impairment in the myelination process. The number and size of myelinated segments was determined, as well as, the paranodal length (the distance between two adjacent myelin segments). The results showed a drastic decrease in the number of myelin segments (Figure 16 B). In addition, the length of myelinated segments was also assessed and the absence of plasmalogen affected this feature in which *Gnpat* KO mice exhibited shorter myelinated segments (Figure 16 C) and an increase in the paranodal distance (Figure 16 D). The latter observation corroborated the results obtained with Caspr labelling in teased fibers, indicating a defect in nodal assembly.

IMPAIRED SIGNALLING PATHWAYS DURING MYELINATION PROCESS

With the detailed characterization of the neuropathy caused by the deficiency in plasmalogens, we aimed at understanding the mechanisms behind the pathology. Based on the phenotype and pathology we decided to study the expression levels of several kinases in 15-day old WT and *Gnpat* KO mice. The choice of age was a compromise between younger ages, in which we may not have sufficient material from individual mice, and older ages, in which the peak of the signalling pathways involved in radial sorting and myelination has passed.

The expression levels of phosphorylated (active) ERK1/2, AKT, JNK and STAT-3 were evaluated by western blot. The levels of phosphorylated ERK1/2, JNK and STAT-3 in sciatic nerve lysates from *Gnpat* KO mice were similar to those of WT nerves (Figure 17). Nevertheless, we found that the levels of phosphorylated AKT (at Ser473 and Thr308) were significantly reduced in nerve lysates from *Gnpat* KO mice (Figure 18 A). To determine if the reduction in active AKT, would impact on the phosphorylation of its targets we analysed the expression of phosphorylated GSK3 β and c-Raf. The levels of phosphorylated GSK3 β at Ser9 (Figure 18 B) and phosphorylated c-RAF at Ser259 (Figure 18 C), were reduced in nerve lysates from *Gnpat* KO mice. Combined, these results indicate that in sciatic nerves from P15 *Gnpat* KO mice, there is an impairment in AKT-mediated signalling.

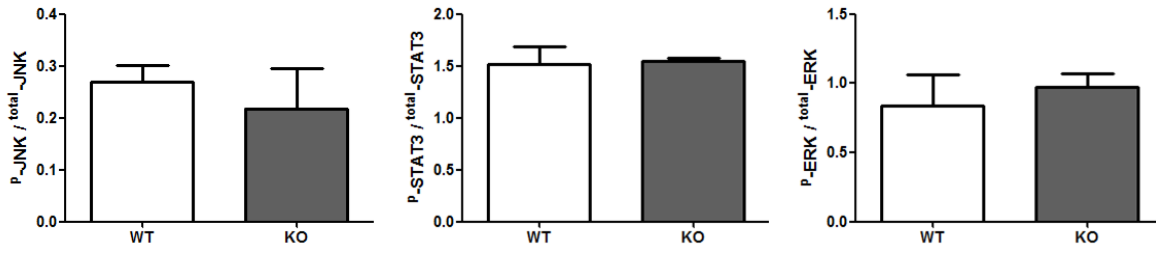


Figure 17. Plasmalogen deficiency does not affect the activation of JNK, STAT3 and ERK1/2. Sciatic nerve lysates from P15 WT and Gnpat KO mice were analyzed by Western Blot for the expression of phosphorylated forms of JNK, STAT3 and ERK1/2. When compared with WT, plasmalogen deficient mice did not exhibit alterations in the phosphorylation status of these three kinases. Error bars show s.e.m.

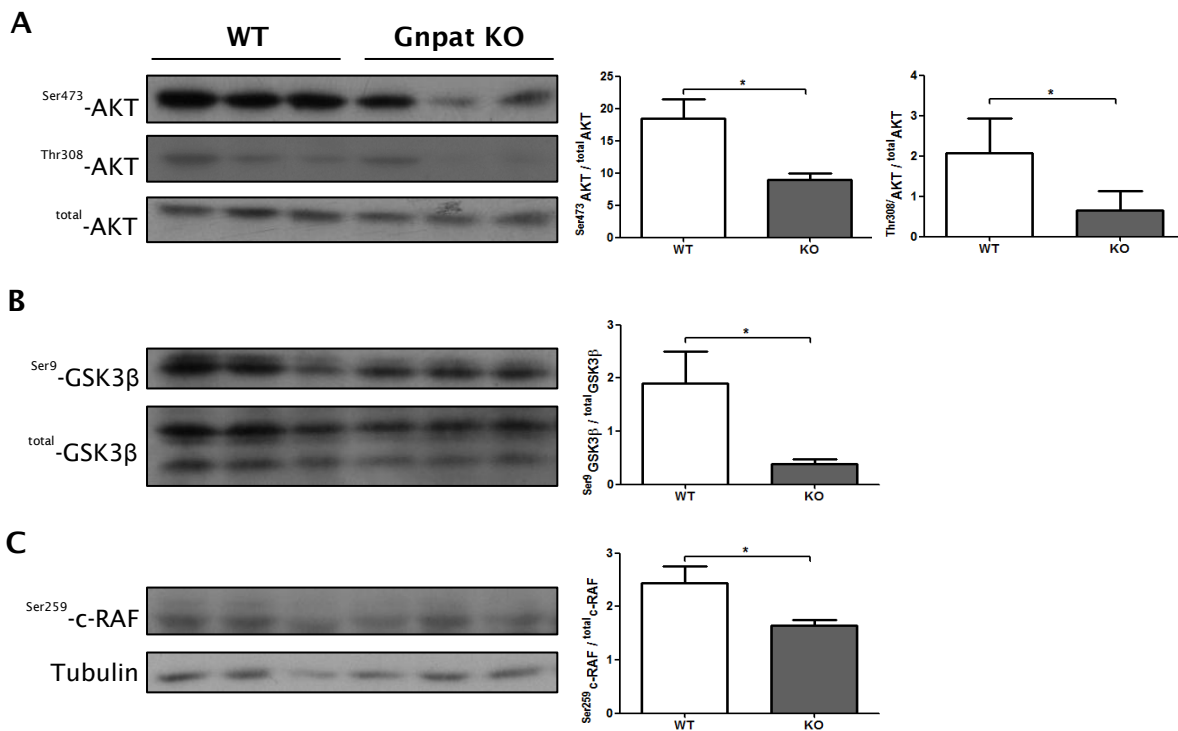


Figure 18. Plasmalogen deficient mice show an altered phosphorylation status of AKT and two of its downstream targets, GSK3β and c-RAF. Sciatic nerve lysates from P15 WT and Gnpat KO mice were analyzed by Western Blot for the expression of phosphorylated forms of AKT, GSK3β and c-RAF. Both phosphorylated forms of AKT (Ser473 and Thr308) were decreased as well as GSK3β phosphorylated in the Ser9 and c-RAF phosphorylated in the Ser259. Statistical analysis was performed using Students T-test. Error bars show s.e.m. and * = $p < 0.05$.

Of interest, is the observation that impaired AKT activation, leads to reduced levels of GSK3 β phosphorylated at Ser9. Previously, it has been shown that upon phosphorylation and activation AKT phosphorylates GSK3 β at Ser9, rendering GSK3 β inactive. This inactivation of GSK3 β is crucial during the process of myelination as it is necessary to allow the transition of Schwann cells from immature to pro-myelinating, in the processes of radial sorting and initiation of myelin formation [89]. As such, our results seem to explain the pathological findings in nerves from Gnpat KO mice and place AKT and GSK3 β as potential targets and/or effectors in a plasmalogen deficiency.

DEFICIENT AKT PATHWAY ACTIVATION IN PLASMALOGEN ABSENCE

Given that plasmalogen-deficient nerves have an impaired activation of AKT and an impaired AKT-mediated signalling cascade, we next aimed at characterizing in more detail the defect in the AKT activation.

To determine if the defect in AKT activation was cell specific and/or specific to a given receptor or a specific signalling cascade, we investigated if mouse embryonic fibroblasts (MEFs) from WT and Gnpat KO mice, would respond similarly to serum stimulation [104]. For this, MEFs were starved O/N and then stimulated with 10% FBS for 0, 1, 3 and 5 minutes. In WT MEFs, AKT activation was time dependent, reaching a maximal response after 5 min of FBS stimulation (Figure 19 A). However, in plasmalogen-deficient MEFs we observed a defective activation of AKT, with reduced levels of phosphorylation at Ser473 and Thr308 (Figure 19 B and C). The impairment in AKT activation seems specific as the FBS stimulus is able to normally activate ERK1/2 in MEFs from Gnpat KO mice (Figure 19 D and E).

Combined, these results indicated that regardless of the cell type and stimuli, a deficiency in plasmalogens results in a specific impairment in AKT phosphorylation.

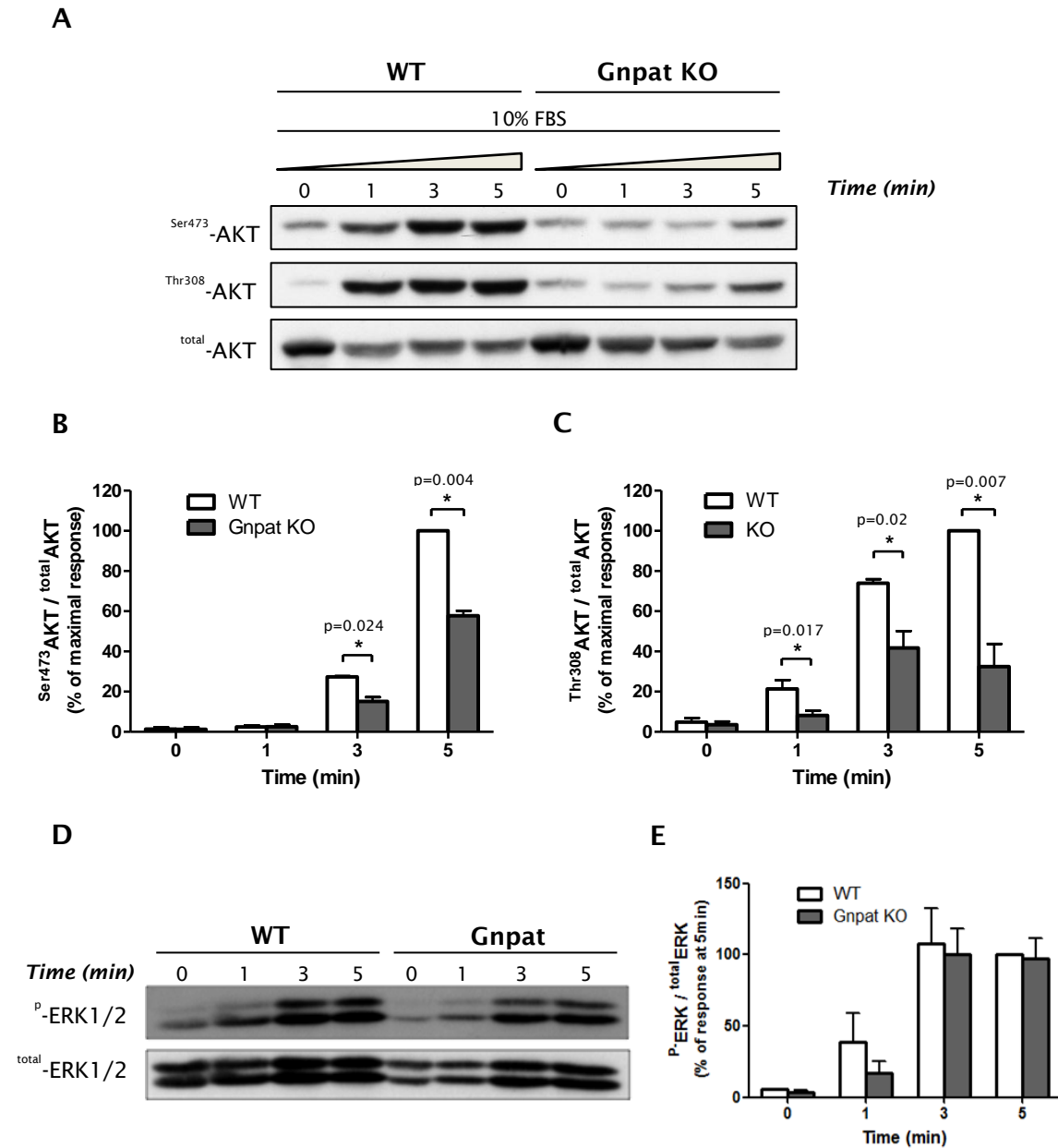


Figure 19. Absence of Plasmalogens interferes with AKT activation in Gnpat KO MEFs. Serum-starved WT and Gnpat KO MEFs were stimulated with 10% FBS for 0, 1, 3 and 5 min. Lysates were prepared from each individual point and western blot analysis of AKT phosphorylation was performed (A). For the quantification of phosphorylated levels of AKT, averaged values of 3 independent experiments are shown as percentage of the maximal levels of phosphorylation found in WT MEFs (B, C). As control we determined the degree of ERK1/2 phosphorylation after FBS stimulation (D, E). Statistical analysis was performed using Mann-Whitney test, and significant P values are shown above bars. Error bars show s.e.m.

LACK OF PLASMOLOGENS IMPAIRS MEMBRANE RECRUITMENT OF AKT

AKT activation requires the phosphorylation of Ser473 and of Thr308, but for this phosphorylation to occur, AKT must be recruited to the plasma membrane [105]. Given that we observed that a plasmalogen deficiency impairs AKT activation in a cell/tissue- and stimuli-independent manner, we hypothesized that the reduced phosphorylation and activation of AKT in plasmalogen-deficient cells could be due to an impairment in AKT recruitment to the plasma membrane.

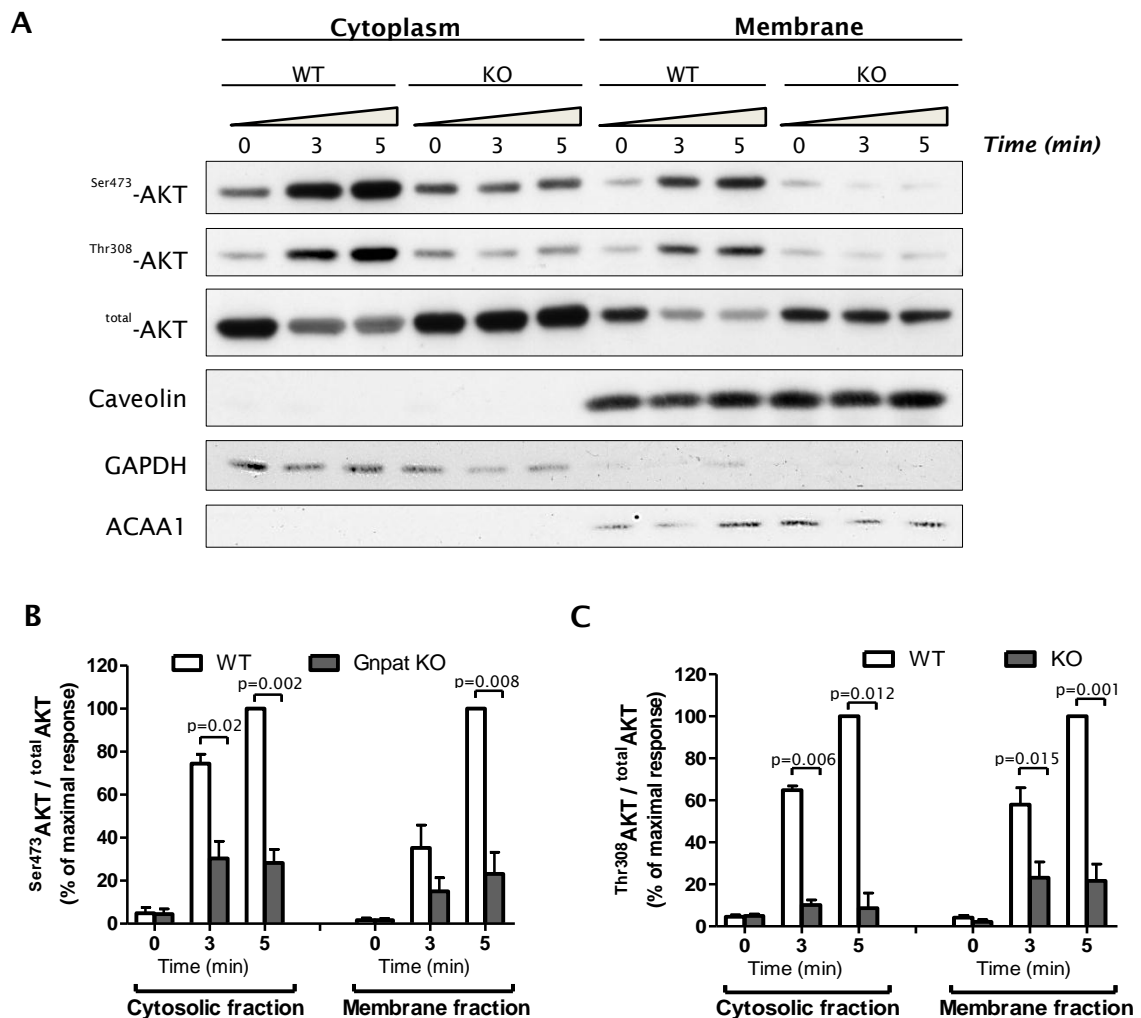


Figure 20. Plasmalogen deficiency leads to impaired recruitment of AKT to the plasma membrane. Serum-starved WT and Gnat KO MEFs were stimulated with 10% FBS for 0, 3 and 5 min. Lysates were prepared from each individual point and western blot analysis of AKT phosphorylation was performed (A). Additionally, three different intracellular markers were analysed to evaluate the purity of the fractions: Caveolin, GAPDH and ACAA1. For the quantification of phosphorylated levels of AKT, averaged values of 3 independent experiments are shown as percentage of the maximal levels of phosphorylation found in WT MEFs (B, C). Statistical analysis was performed using Mann-Whitney test, and significant P values are shown above bars. Error bars show s.e.m.

Using MEFs from WT and Gnpat KO mice and FBS stimulation setup, we performed differential permeabilization and extraction of proteins to obtain different subcellular fractions. Serum starved MEFs were stimulated with 10% FBS for 0, 3 and 5min, and lysates from these time points were used to analyse AKT phosphorylation in cytosolic and membrane fractions (Figure 20 A). In WT MEFs we observed the time-dependent increase in the phosphorylated forms of AKT in the cytosolic and membrane fractions (Figure 20 B and C).

However, in Gnpat KO MEFs, we observed reduced levels of membrane-associated AKT and reduced AKT phosphorylation in both cytosolic and membrane fractions (Figure 20 B and C). To control for purity of the fractions and the strength of differential extraction, we analysed the levels of caveolin-1 (a membrane marker), GAPDH (a cytosolic marker) and ACAA1 (a peroxisomal marker) (Figure 18A). The presence of caveolin-1 and GAPDH in their corresponding fractions confirmed the ability of the differential protein extraction. In addition, and given that AKT is weakly associated with the plasma membrane, we verified that the extraction performed to obtain the cytosolic proteins would not interfere with membrane solubilization (that could release proteins that are weakly associated with membranes). The localization of ACAA1, a peroxisomal protein localized to the matrix of the organelle, was restricted to the membrane fractions (Figure 20 A), indicating that the extraction of cytosolic proteins does not have enough strength to interfere with proteins loosely associated with membranes.

INHIBITION OF GSK3 β RESCUES PNS DEFECTS OF PLASMALOGEN-DEFICIENCY

The characterization of the mechanism behind the deficiency in plasmalogens, revealing that AKT-mediated signalling is impaired in nerves from Gnpat KO mice, allowed us to devise and test a potential therapeutic intervention. Given that GSK3 β is a known negative regulator of Schwann cell differentiation and myelination, and that we found decreased levels of the inactive form of GSK3 β (phosphorylated at Ser9), we hypothesized that pharmacological or

chemical inhibition of GSK3 β would be able to improve the impaired processes of mutant Schwann cells.

Lithium chloride (LiCl) is a well known inhibitor of GSK3 β , and is currently used for the treatment of bipolar disorders and mood alterations [106], [107]. The mechanism of action of LiCl in the inhibition of GSK3 β is rather complex [108], as it may act directly on GSK3 β or preventing the dephosphorylation of AKT by protein phosphatase 2A [109]. Therefore we first determined if the *in vitro* defect in myelination observed in co-cultures of Gnpat KO mice, could be modulated by LiCl. DRG co-cultures of neurons and Schwann cells were prepared from WT and Gnpat KO mice, and LiCl was added to the culture 4 days before the initiation of myelination, as not to interfere with neurite formation or growth.

Comparing to the control treatment (16mM NaCl), in which we observe a striking myelination defect in Gnpat KO co-cultures, the addition of LiCl was able to completely rescue myelination in the absence of plasmalogens in which the co-cultures presented an increase in the number of myelin positive segments (Figure 21).

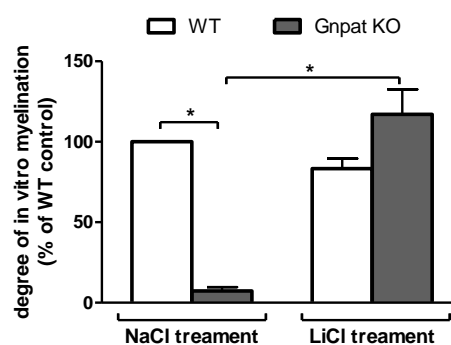


Figure 21. LiCl treatment is able to revert the defect in myelination in plasmalogen deficient mice. Treatment with LiCl was able to rescue the myelination defect in DRG co-cultures of neurons and Schwann cells from Gnpat KO embryos. The degree of *in vitro* myelination was determined as the density of myelin segments (positive for MBP) 11 days after the daily addition of ascorbic acid in medium supplemented with 16mM NaCl (control) or with 16mM LiCl. Statistical analysis was performed using one-way ANOVA. Error bars show s.e.m. and * = $p < 0.05$.

The results obtained showing a rescue of *in vitro* myelination with addition of LiCl, prompted the determination if *in vivo* treatment with LiCl could also lead to an improvement or rescue of the pathology. We devised 2 treatment schemes: on setup A, we initiated subcutaneous injections of LiCl at a dosage of 50mg/Kg

on alternating days from P7 to P15; on setup B, we initiated daily subcutaneous injections of LiCl at a dosage of 50mg/Kg from P1 to P6.

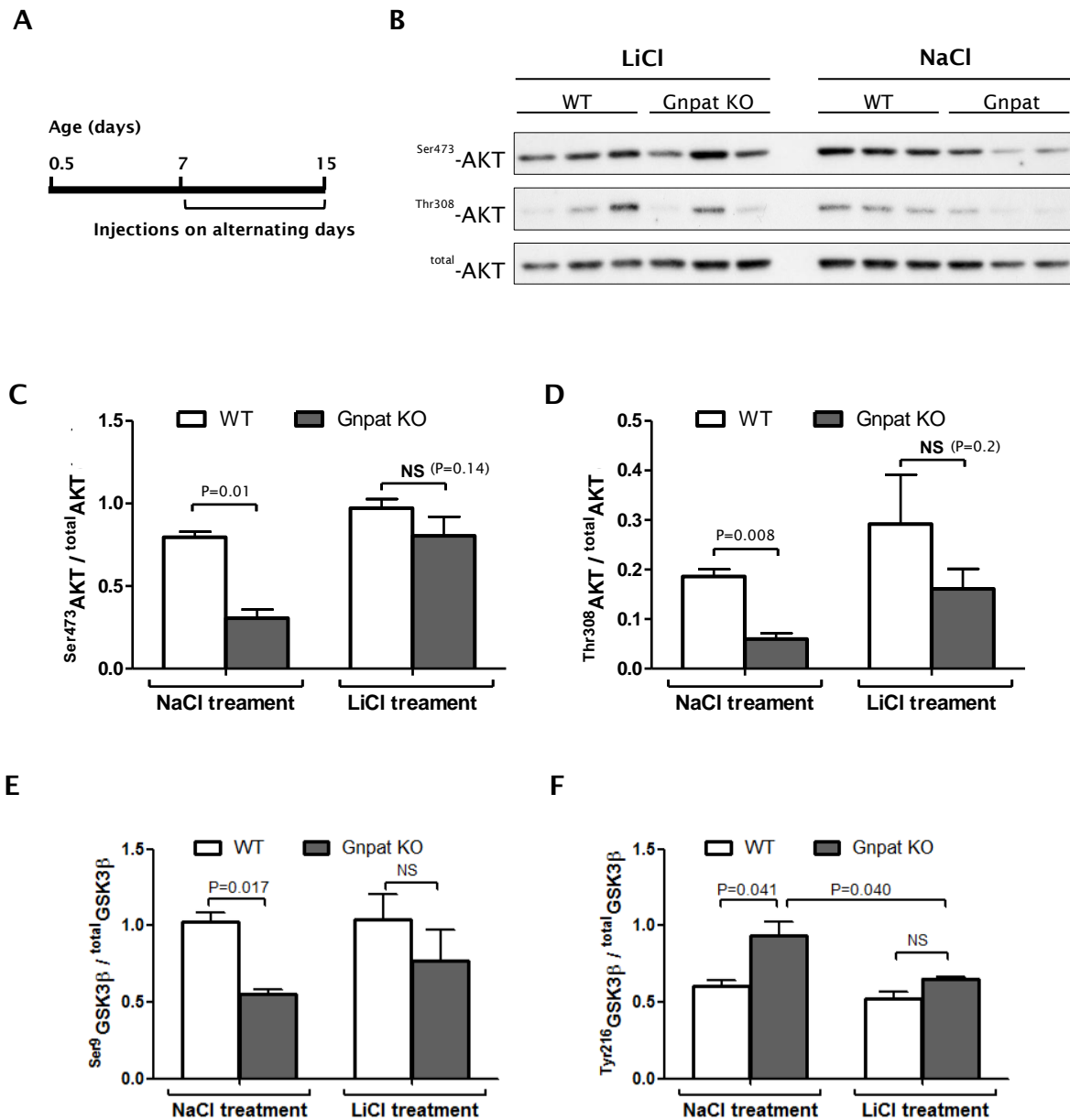


Figure 22. LiCl restores AKT activation and GSK3β inhibition in Gnpat KO mice. Sciatic nerve lysates from P15 WT and Gnpat KO mice treated with LiCl were analyzed by Western Blot for the expression of phosphorylated forms of AKT and GSK3β. LiCl treatment according to setup A was able to restore AKT phosphorylation levels at both Ser473 and Thr308 (B-D). Moreover, inhibitory phosphorylation of GSK3β at Ser9 increased with LiCl treatment (E) and the active form of GSK3β phosphorylated at Tyr216 was decreased (F). Statistical analysis was performed using Mann-Whitney test and significant p values are shown above bars. Error bars show s.e.m.

Western blot analyses in nerve lysates from P15 mice treated according to setup A, revealed an increase in the phosphorylation levels of AKT in nerves from LiCl-treated Gnpat KO mice, that reached the levels observed in WT mice (Figure 22 B to D). Concomitant with the increase in active AKT, we observed an increase in the inhibitory phosphorylation at Ser9 of GSK3 β (Figure 22 E), and a decrease in the active form of GSK3 β , i.e., GSK3 β phosphorylated at Tyr216 (Figure 22 F).

Combined, these results suggested that LiCl treatment in Gnpat KO mice was able to rescue the biochemical and signalling defect caused by the lack of plasmalogens.

Given that the treatment with LiCl was able to restore AKT-mediated signalling in plasmalogen-deficient nerves, we investigated if this would have beneficial outcomes during the period of axonal sorting, to rescue the observed defects in Gnpat KO mice. Western blot analyses in muscle lysates from P6 mice treated according to setup B, revealed an increase in the phosphorylated form of GSK3 β at Ser9, indicative of AKT-mediated signalling activation and concomitant inactivation of GSK3 β (Figure 23 B and C).

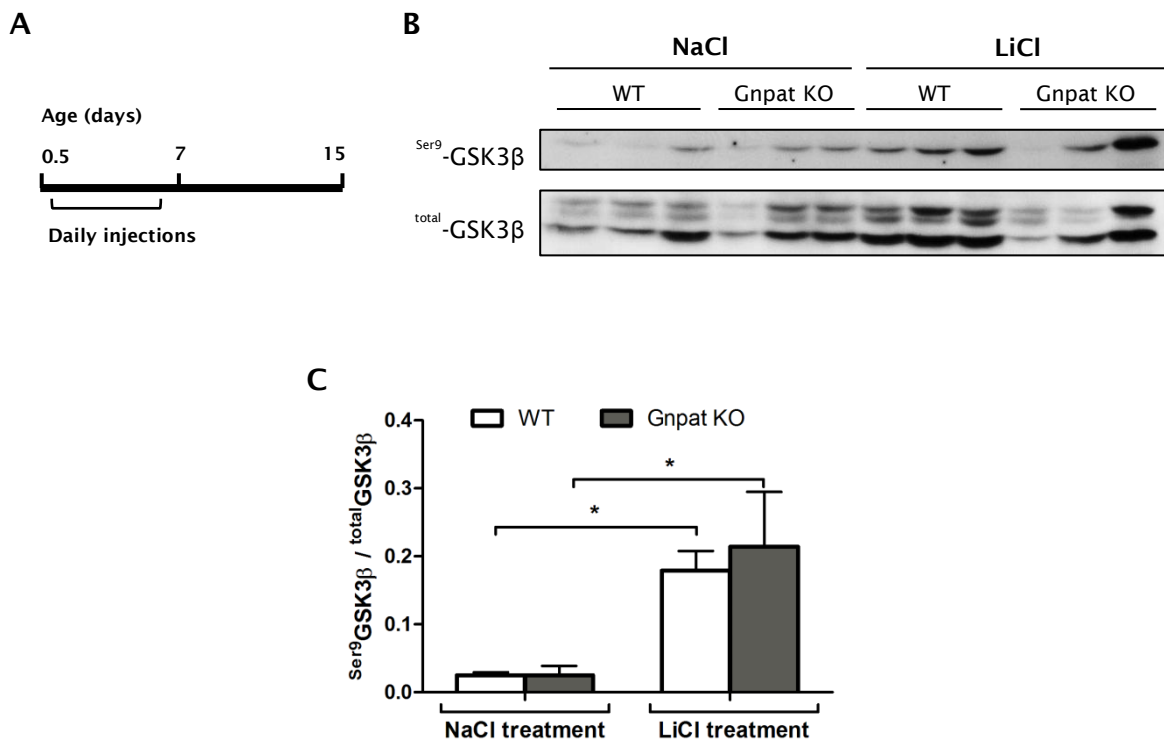


Figure 23. LiCl treatment inactivates GSK3 β in the period of axonal sorting. Muscle lysates from P6 WT and Gnpat KO mice treated with LiCl were analyzed by Western Blot for the expression of phosphorylated form of GSK3 β at Ser9. LiCl treatment according to setup B was able to inhibit GSK3 β by increasing its phosphorylation at Ser9 (B, C). Statistical analysis was performed using Mann-Whitney test. Error bars show s.e.m. and * = $p < 0.05$

The treatment with LiCl was also able to restore Schwann cell differentiation in nerves from P6 Gnpat KO mice, as we observed a decrease in the levels of Sox2, a marker of immature Schwann cells (Figure 24 A) and an increase in Oct6, a marker of differentiated myelinating Schwann cells (Figure 24 B).

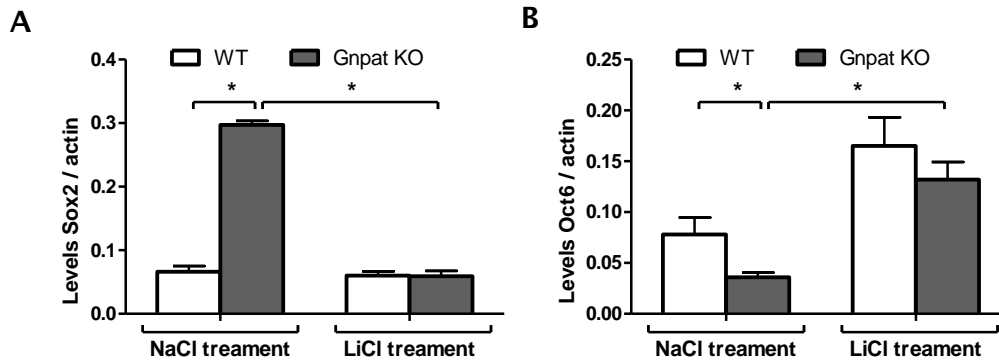
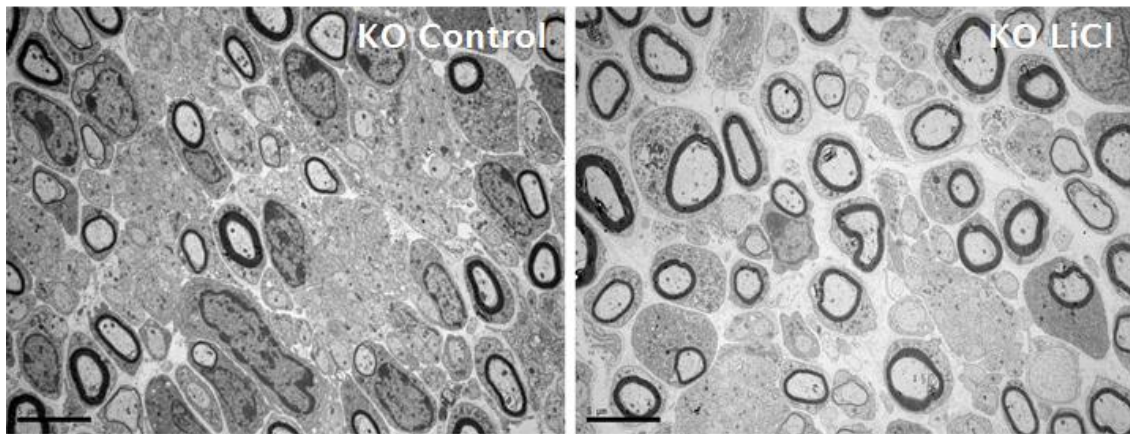


Figure 24. LiCl treatment restores Schwann cell differentiation. Western Blot assays performed in sciatic nerves from Setup B treated mice exhibited decreased levels of Sox2 indicative of a reduction in the immature state of the nerve (A). Furthermore, Oct6 levels rose above the control conditions in both WT and Gnpat KO mice demonstrating increased levels of differentiated Schwann cells in the myelinating nerve (B). Statistical analysis was performed using Mann-Whitney test. Error bars show s.e.m. and * = $p < 0.05$.

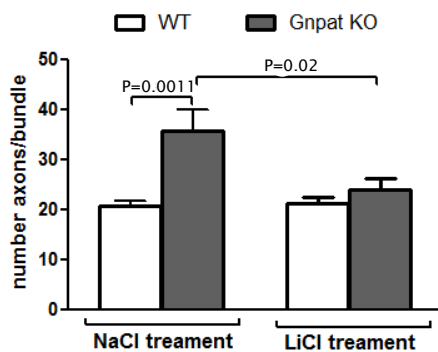
Given that our biochemical assessment indicated that the LiCl treatment was able to rescue the impaired signalling and the differentiation of the Schwann cell, we investigated if this improvement would have a beneficial outcome in terms of the pathophysiology of sciatic nerves from P6 mice (setup B). Ultrastructural analysis of sciatic nerves from control-treated and LiCl-treated Gnpat KO mice, revealed a striking effect of LiCl administration (Figure 25). Whereas nerves from control-treated KO mice, showed the characteristic hypomyelination, LiCl treatment, and in accordance with the levels of Oct6 (Figure 24), was able to induce myelination and restore the histological appearance of sciatic nerves (Figure 25 A).

In order to have a better assessment on the beneficial consequences of LiCl, we determine: 1- the number of axons per bundle, to evaluate if the treatment would rescue the defect in axonal sorting; and 2- the density of sorted axons/promyelinating Schwann cells, to evaluate the differentiation of Schwann cells.

A



B



C

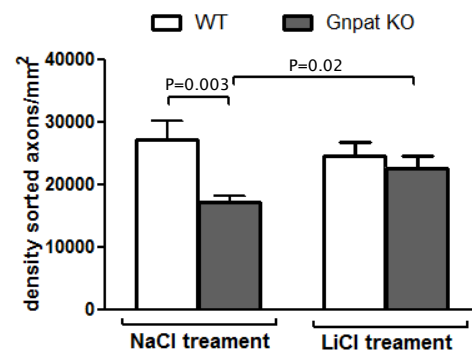


Figure 25. LiCl treatment rescues radial sorting and myelination. Electron microscopy assessment of P6 *Gnat* KO nerves treated with LiCl revealed an apparent recovery in the myelination (A). Further evaluation showed that LiCl treatment leads to a normalization in the number of axons per bundle (B) and in the density of sorted axons (C). Statistical analysis was performed using Student's t-test and significant p values are shown above bars. Error bars show s.e.m. Scale bar = 5 μ m.

The results obtained showed that upon LiCl treatment there was a normalization in the number of axons/bundle, since in sciatic nerves from LiCl-treated mice there was a significant reduction in the number of these unsorted axons to normal values (Figure 25 B). In addition, we also observed a significant increase in the density of sorted axons, in LiCl-treated KO mice indicating a normal progression of Schwann cells from immature to pro-myelinating stage (Figure 25 C).

Combined, the results demonstrate the efficacy of LiCl treatment in restoring the impaired signalling pathway, and in improving the development of mutant Schwann cells, which leads to a rescue in radial sorting and myelination.

CHAPTER V

DISCUSSION

Plasmalogens are a special class of phospholipids, as they contain a vinyl-ether bond at the *sn-1* position of the glycerol backbone [2], [3], [5]. This feature is thought to be responsible for some of the functions attributed to plasmalogens which include antioxidant properties and determinants of membrane fluidity [11], [29]. In addition, and due to their composition, plasmalogens are also thought to serve as storage of PUFAs and sources of lipid mediators, through the metabolism of PUFAs [3]. The importance of plasmalogens in health is best understood from the disease perspective, as a deficiency in the biosynthesis of plasmalogens is the cause of RCDP, a developmental disorder with defects in bone, brain, and eye development. In addition, other disorders, including Zellweger syndrome, Alzheimer's disease, X-linked adrenoleukodystrophy have defects in plasmalogens which are thought to modulate the disease presentation and progression [3]. As plasmalogens are highly enriched in the nervous tissue, and given that in most human disorders with defects in plasmalogens, neurodegeneration is a feature of the disease, it is important to understand the consequences of plasmalogen defects to nervous tissue. Our main aim was to determine the role and importance of plasmalogens in the myelination of the peripheral nervous system, through the assessment of the phenotypic presentation and sciatic nerve pathology of knockout mice with defects in the biosynthesis of plasmalogens.

Previous work at the Nerve Regeneration group, has revealed that a deficiency in plasmalogens impairs the initial stages of myelination, through a dual process: (1) - defects in plasmalogens impair the process of radial sorting, leading to the accumulation of large calibre axons in bundles, which fail to be segregated for myelination; and (2) - defects in plasmalogens impair the myelination process, as sorted axons showed increased g-ratio, indicative of less myelin. Despite this initial defect, we observed a normal degree of myelination in sciatic nerves from adult knockout mice. This led us to raise two main questions: despite the normal amounts of myelin in nerves from adult knockout mice, is the organization of myelin and the myelinating Schwann cell normal? Does a plasmalogen deficiency affect myelin maintenance in aged mice?

Using our approach, the phenotypic characterization of plasmalogen-deficient mice revealed that plasmalogen-deficient mice acquired an age-dependent neuropathy, as they developed ataxia and tremors. On average, the knockout mice reached a humane end point at 17 months of age, as the severity

of ataxia progressed from locomotion and gait impairments to hindlimb paralysis, and from tremors to a comatose-like state. Histological and ultrastructural analyses of sciatic nerves from aged knockout mice revealed a severe demyelination and axonal loss. Demyelination was evident not only by the thinning of the myelin sheath but also by the presence of axons completely devoid of myelin. Probably in an endeavour to remyelinate, we observed that Schwann cells from knockout mice produced and extended processes to attempt to engulf demyelinated axons and initiate the remyelination process. Nevertheless, the endoneurium of sciatic nerves from plasmalogen-deficient mice is filled with these processes, and we observed that even non-myelinating Schwann cells (forming the Remak bundle) extended these processes, and what appears to be still normally myelinated axons, contain several processes around them. Combined, our results indicate that a plasmalogen deficiency impairs the Schwann cell ability to maintain myelin and to respond to demyelination (Figure 26). The reason behind this is currently unknown, although given the role of plasmalogens as antioxidants and the increase in oxidative stress with age, it might be possible that the lack of plasmalogens renders myelin more prone or sensitive to oxidative damage leading to demyelination. Future work should include the measurement of oxidative stress markers, to determine if an accumulation of oxidative damage is behind the loss of myelin. Nevertheless, our results showed that before the onset of demyelination, sciatic nerves from knockout mice are dysmyelinated, *i.e.*, despite having normal myelin thickness the organization of myelin is abnormal. We observed that plasmalogen-deficient myelin has a greater number of Schmidt-Lanterman incisures and a disruption of Schwann cell appositions. The abnormal cytoarchitecture of the mutant Schwann cells also caused some abnormalities in axons, as we observed a diffuse localization of Caspr, which is normally localized to the paranode. Combined, our results indicate that in the absence of plasmalogens, Schwann cells are able to produce normal amounts of myelin, but its structure and organization is abnormal. This defect may not only contribute to the reduced nerve conduction but also to decreased myelin stability, which may modulate the demyelination we observed in aged mice.

In order to attain a deeper understanding of how a plasmalogen deficiency causes impaired radial sorting and myelination, we set out to determine the cellular changes in terms of signalling pathways. For this we used lysates of

sciatic nerves from 15 days old WT and knockout mice, which we probed by western blot for the expression of several key kinases. From our small screen analyses, we identified AKT as a kinase that is differentially phosphorylated in sciatic nerve lysates from knockout mice. Receptor-mediated activation of AKT is mediated by its translocation from the cytosol to the membrane, where it is phosphorylated at Ser473 and Thr308 [105]. Upon phosphorylation, active AKT shuttles back to the cytosol where it can phosphorylate a myriad of substrates [110]. The phosphorylation by AKT can be either inhibitory or activating depending on the target and the residue that it phosphorylates. From the myriad of AKT substrates we analysed two, namely c-RAF and GSK3 β , as they could have a role to play in the pathology observed in nerves from plasmalogen-deficient mice. GSK3 β has a non-myelinating effect which prevents the passage of Schwann cells from immature to a pro-myelinating stage, thus mediating both axonal sorting and myelination itself [89]. During normal postnatal development, GSK3 β needs to be phosphorylated by AKT at Ser9 in order to be inactivated and allow the differentiation and maturation of Schwann cell to myelin-producing glia. When c-RAF is phosphorylated by AKT at the highly conserved Ser259, it acquires an inactive state [111] becoming unable to perform its kinase activity and, this way, interfere with myelination [74]. In our analysis, combined with the reduced phosphorylation of AKT, we observed a reduced phosphorylation of GSK3 β at Ser9 and c-RAF at Ser259. As such, our results indicate that a deficiency in plasmalogens causes impaired AKT-mediated signalling, and that GSK3 β and c-RAF may play a role in the cellular changes that cause impaired radial sorting and myelination (Figure 26).

In order to understand how a plasmalogen deficiency could affect AKT activation and its signalling pathway, we investigated AKT activation in detail. We hypothesised that a defect in AKT activation could be either, receptor/ligand-mediated or receptor/ligand-independent. In the former hypothesis, a plasmalogen deficiency could affect receptor localization, its interaction with a given ligand or its activation (e.g. by dimerization), which would not initiate a signalling cascade failing to phosphorylate AKT. This hypothesis predicted that a plasmalogen deficiency would cause impairments in receptor/ligand interactions and functions, in a way that is specific for each cell type and tissue. In Schwann cells impaired NRG1 signalling via ErbB2/3 would cause reduced AKT activation, but in neurons the receptor affected would be different, and the same would be

true for all the tissues where a plasmalogen deficiency causes pathology. This would imply that in every tissue/cell with a plasmalogen deficiency (ranging from eye, testis, bone, neurons, to harderian gland and adipose tissue) a different receptor would be affected. Therefore we wondered if a plasmalogen deficiency would cause a receptor/ligand-independent defect in AKT activation. In this scenario, we hypothesized that a plasmalogen deficiency would impair AKT phosphorylation down-stream of receptor activation, in a cell type and tissue independent manner, and could explain the myriad of cellular defects and tissue pathology in RCDP patients and knockout mice.

Our results showed that the impaired AKT activation is cell-independent, as MEFs from *Gnpat* knockout mice also had reduced levels of phosphorylated AKT. In addition, we showed that upon serum stimulation MEFs from *Gnpat* knockout mice were unable to activate the AKT-mediated signalling cascade, but they were able to induce ERK1/2 activation. These results suggested that our hypothesis of a receptor/ligand-independent defect in AKT activation would be behind a plasmalogen deficiency. For AKT to be phosphorylated and activated, unphosphorylated AKT needs to associate with the plasma membrane. As such, there is a shuttle of AKT from the cytosol to the membrane and back to the cytosol to phosphorylate its target proteins. We hypothesized that a defect in plasmalogens could impair the association of AKT to the membrane, and therefore block AKT phosphorylation. Using differential permeabilization and protein extraction, we found extremely reduced levels of AKT phosphorylation in the membrane fraction of MEFs from *Gnpat* knockout mice, suggesting either a defect in the kinases that phosphorylate AKT or in its ability to become membrane associated with subsequent phosphorylation. Our preliminary results (data not shown) revealed that the levels of PDK1 and PTEN are normal in sciatic nerve lysates from knockout mice, suggesting that a deficiency of plasmalogens at the plasma membrane impairs AKT activation and its signalling pathway.

Recently, it has been shown that feeding an alkyl-glycerol to *Pex7* knockout mice is able to rescue the defect in biosynthesis of plasmalogens, as alkyl-glycerol serves as an alternative precursor [112]. In several tissues (e.g. liver, kidney, eye, testis and heart) the alkyl-glycerol treatment normalizes the levels of plasmalogens and is able to prevent or halt the pathological alterations. Nevertheless, the treatment was inefficient in rescuing the levels of plasmalogens in nervous tissue. In our work, the unravelling of the mechanism behind a

plasmalogens deficiency in the peripheral nervous tissue, allowed us to devise and test a therapeutic intervention aimed, not at restoring plasmalogen levels but at rescuing the impaired signalling pathway.

As discussed above, GSK3 β is thought to play an important role during radial sorting and myelination. Given our results, we hypothesized that chemical or pharmacological inhibition of GSK3 β would be able to circumvent the impaired inhibitory phosphorylation at Ser9, and allow the differentiation of Schwann cells. We have investigated if treatment with lithium chloride (LiCl) would have beneficial effects, as lithium is widely used to treat neurological diseases such as bipolar conditions and is a well described GSK3 β inhibitor [89], [109], [106], [107].

As the addition of LiCl, to *in vitro* myelinating co-cultures of DRG neurons and Schwann cells from knockout mice, resulted in a rescue of myelination, we initiated *in vivo* studies at two different developmental stages. To determine that the LiCl treatment would have a positive outcome in the AKT-mediated signalling pathway we determined the levels of phosphorylated AKT in sciatic nerves from 15 days old WT and knockout mice. Our results showed that the administration of LiCl for 8 days was able to increase the levels of phosphorylated AKT. LiCl has a complex and wide range of action [108], and our results confirm that in addition to the expected direct inhibitory effect on the activity of GSK3 β , LiCl is also able to increase the levels of phosphorylated AKT (possibly by inhibiting the phosphatase PP2a) [109], which may result in a further inhibitory action on GSK3 β by AKT-mediated phosphorylation at Ser9. To determine if LiCl administration would be able to rescue the defects in axonal sorting and myelination, we investigated if treatment with LiCl would be therapeutic during the active period of radial sorting and initial stages of myelination [89]. Western blot analysis of muscle lysates from 6 days old WT and Gnatp knockout pups, revealed that LiCl administration was able to increase GSK3 β phosphorylation at Ser 9 by 7-fold. The treatment with LiCl was also able to induce differentiation of mutant Schwann cells, as we observed a decrease in the levels of Sox2 with a concomitant increase in the levels on Oct6. Sox2 is a negative myelination regulator and is overexpressed in nerve injury and in other scenarios in which the myelination process is impaired [65]. Being characteristic of the immature stage of the SC, its decrease in the LiCl treated condition leads to conclusion that the treatment might be effective. Oct6 is a positive myelination marker and acts in union with

Sox10 to activate Krox20 which is a pro-myelination transcription factor [113]. The increased levels of Oct6 together with the decreased levels of Sox2 combined with the ultrastructural analysis, showed an improvement in Schwann cell differentiation and maturation with increase in the myelination status of sciatic nerves from LiCl-treated Gnat KO mice. Quantitative analyses of axonal density in bundles and sorted axons with pro-myelinating Schwann cells revealed that the treatment with LiCl was able to rescue the defect in radial sorting present in knockout mice.

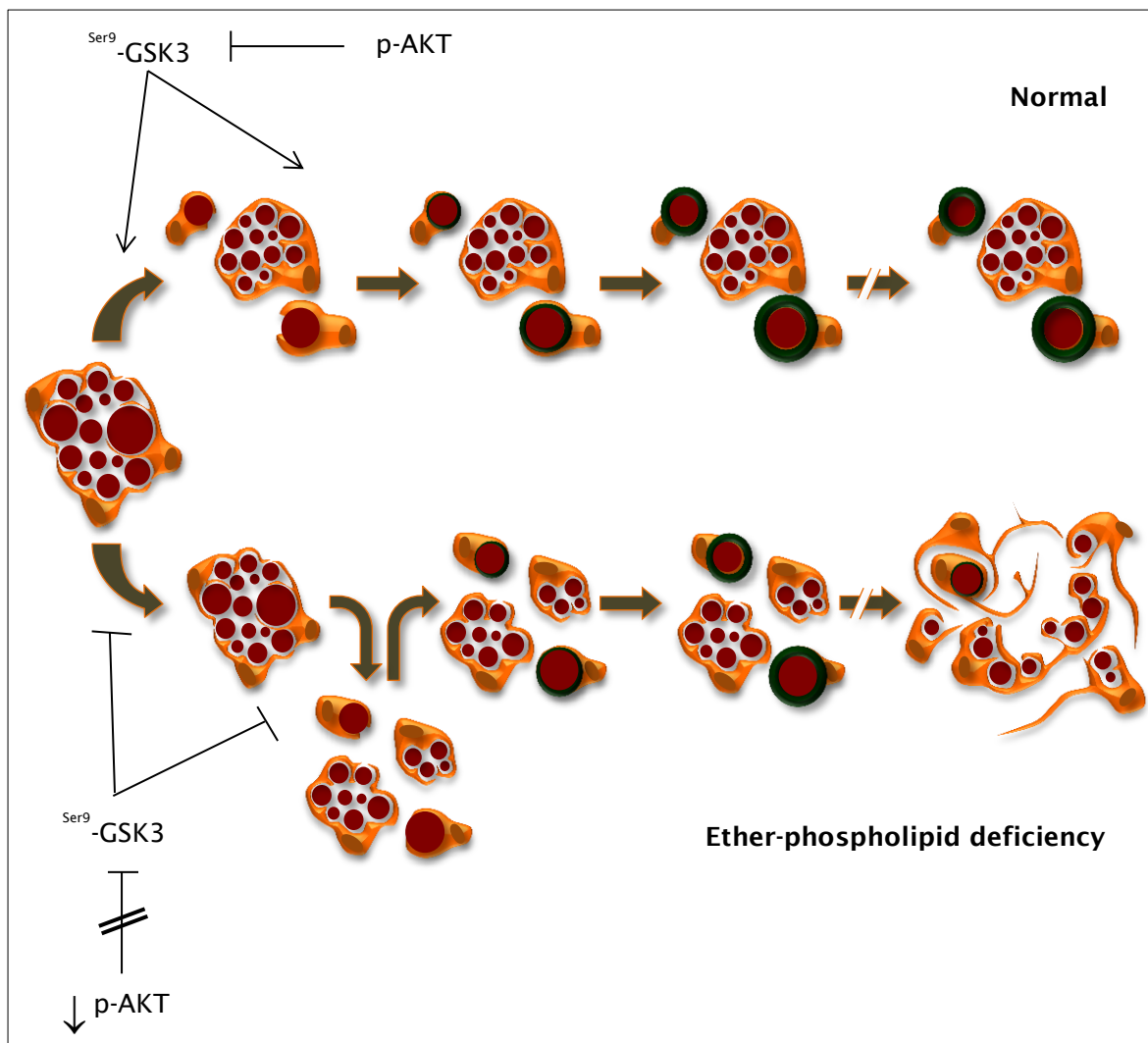


Figure 26. Summarized model representing the pathology and mechanisms inherent to plasmalogen deficiency. In WT condition (upper panel; normal) there is a normal myelination process with an initial functional radial sorting accompanied by a normal AKT-mediated signalling pathway which leads to GSK3 β inhibition. On the other hand, plasmalogen deficiency (lower panel; ether-phospholipid deficiency) presents an impaired signalling pathway with a decrease in GSK3 β inactivation and a concomitant impairment in radial sorting and initial stages of myelination. Lack of plasmalogens leads, in adult stages, to normal amount of myelin but abnormally formed and, with aging, to a demyelination phenotype accompanied by axon loss.

C

CHAPTER VI

CONCLUSIONS

As final remarks, we can effectively assign important roles of plasmalogens in Schwann cells and to the myelination process. Although plasmalogens have been associated with regulation of membrane fluidity and with scavenging reactive oxygen species, we showed that they may also play an important role as determinants or mediators of the transient association that some proteins establish with the plasma membrane. Our studies revealed that plasmalogens enable the membrane association of AKT with its subsequent activation. In the peripheral nervous system, a deficiency in plasmalogens impairs AKT-mediated signalling, causing defects in axonal sorting and myelination in a GSK3 β -mediated process. The plasmalogen deficiency causes initially a hypomyelination of the PNS, which develops into a status of dysmyelination with roughly normal amounts of abnormally formed myelin. The combination of abnormally structured myelin with increased oxidative stress in aged PNS, leads to a severe neuropathy with demyelination and axonal loss.

The defects in nervous tissue caused by a plasmalogen deficiency may not be rescued by treatment with the current alkyl-glycerol therapy, but our determination of the mechanism behind the nerve pathology, allowed us to unravel a new strategy that is able to rescue the axonal sorting and myelination defects. Future work should determine if the treatment with lithium is able to rescue the impaired remyelination in aged mice, and if the combination with alkyl-glycerol treatment is able to yield a truly potent therapeutic intervention to rescue the defects caused by a deficiency in plasmalogens.

REFERENCES

- [1] D. Voet, J. G. Voet, and C. W. Pratt, *Fundamentals of Biochemistry*, 1st ed. John Wiley and Sons, 1999, pp. 223–226.
- [2] N. Nagan and R. a Zoeller, “Plasmalogens: biosynthesis and functions”, *Progress in Lipid Research*, vol. 40, no. 3, pp. 199–229, 2001.
- [3] P. Brites, H. R. Waterham, and R. Wanders, “Functions and biosynthesis of plasmalogens in health and disease”, *Biochimica et Biophysica Acta*, vol. 1636, pp. 219–231, 2004.
- [4] S. Wallner and G. Schmitz, “Plasmalogens the neglected regulatory and scavenging lipid species”, *Chemistry and Physics of Lipids*, vol. 164, pp. 573–589, 2011.
- [5] K. Gorgas, A. Teigler, D. Komljenovic, and W. W. Just, “The ether lipid-deficient mouse: tracking down plasmalogen functions”, *Biochimica et Biophysica Acta*, vol. 1763, pp. 1511–1526, 2006.
- [6] K. Voit and R. Feulgen, “Über einem weitverbreiteten festen Aldehyd”, *Pflüger’s Archiv für die Gesamte Physiologie*, vol. 206, pp. 389–410, 1924.
- [7] R. V. Pangamandala, L. A. Horrocks, J. C. Geer, and D. G. Cornwell, “Positions of double bonds in the monounsaturated alk-1-enyl groups from the plasmalogens of human heart and brain”, *Journal of Chemistry and Physics of Lipids*, vol. 6, pp. 97–102, 1971.
- [8] H. Goldfine, “The appearance, disappearance and reappearance of plasmalogens in evolution”, *Progress in Lipid Research*, vol. 49, no. 4, pp. 493–498, 2010.
- [9] L. A. Horrocks and M. Sharma, “Plasmalogens and O-alkyl glycerophospholipids”, in *Phospholipids, new comprehensive Biochemistry*, J. N. Hawthorne and G. B. Ansell, Eds. Elsevier Biomedical Press, Amsterdam, 1982, pp. 51–93.
- [10] J. Lessig and B. Fuchs, “Plasmalogens in biological systems: their role in oxidative processes in biological membranes, their contribution to pathological processes and aging and plasmalogen analysis”, *Current Medicinal Chemistry*, vol. 16, pp. 2021–2041, 2009.
- [11] A. Hermetter, B. Rainer, E. Ivessa, E. Kalb, J. Loidl, A. Roscher, and F. Paltauf, “Influence of plasmalogen deficiency on membrane fluidity of human skin fibroblasts: a fluorescence anisotropy study”, *Biochimica et Biophysica Acta*, vol. 978, pp. 151–157, 1989.
- [12] T. C. Lee, “Biosynthesis and possible biological functions of plasmalogens”, *Biochimica et Biophysica Acta*, vol. 1394, pp. 129–145, 1998.
- [13] X. Chen and R. W. Gross, “Potassium flux through gramicidin ion channels is augmented in vesicles comprised of plasmenylcholine: correlations between gramicidin conformation and function in chemically distinct host bilayer matrices”, *Biochemistry*, vol. 34, no. 22, pp. 7356–7364, 1995.
- [14] D. Kirschner and A. Ganser, “Myelin labeled with mercuric chloride. Asymmetric localization of phosphatidylethanolamine plasmalogen”, *Journal of Molecular Biology*, vol. 157, pp. 635–658, 1982.

References

- [15] J. A. Post, A. J. Verkleij, B. Roelofsen, and J. A. Op De Kamp, "Plasmalogen content and distribution in the sarcolemma of cultured neonatal rat myocytes", *FEBS letters*, vol. 240, no. 1-2, pp. 78-82, 1988.
- [16] P. Fellmann, P. Hervé, and P. F. Devaux, "Transmembrane distribution and translocation of spin-labeled plasmalogens in human red blood cells", *Chemistry and Physics of Lipids*, vol. 66, no. 3, pp. 225-230, 1993.
- [17] S. E. Thomas, S. J. Morris, D. M. Byers, F. B. Palmer, M. W. Spence, and H. W. Cook, "Polyunsaturated fatty acid incorporation into plasmalogens in plasma membrane of glioma cells is preceded temporally by acylation in microsomes", *Biochimica et Biophysica Acta*, vol. 1126, pp. 125-134, 1992.
- [18] G. Schrakamp, C. G. Schalkwijk, R. B. Schutgens, R. J. Wanders, J. M. Tager, and H. van den Bosch, "Plasmalogen biosynthesis in peroxisomal disorders: fatty alcohol versus alkylglycerol precursors", *Journal of Lipid Research*, vol. 29, pp. 325-334, 1988.
- [19] W. B. Rizzo, D. A. Craft, A. L. Dammann, and M. W. Phillips, "Fatty Alcohol Metabolism in Cultured Human Fibroblasts", *The Journal of Biological Chemistry*, vol. 262, pp. 17412-17419, 1987.
- [20] X. Wang and P. E. Kolattukudy, "Solubilization, purification and characterization of fatty acyl-CoA reductase from duck uropygial gland", *Biochemical and Biophysical Research Communications*, vol. 208, pp. 210-215, 1995.
- [21] H. Hayashi and M. Hara, "1-Alkenyl group of ethanolamine plasmalogen derives mainly from de novo synthesized fatty alcohol within peroxisomes, but not extraperoxisomal fatty alcohol or fatty acid", *Journal of Biochemistry*, vol. 121, pp. 978-983, 1997.
- [22] T.-C. Lee, C. Qian, and F. Snyder, "Biosynthesis of choline plasmalogens in neonatal rat myocytes", *Archives of Biochemistry and Biophysics*, vol. 286, no. 2, pp. 498-503, 1991.
- [23] A. K. Hajra, C. L. Burke, and C. L. Jones, "Subcellular localization of Acyl Coenzyme A : Dihydroxyacetone phosphate acyltransferase in Rat Liver Peroxisomes (Microbodies)", *The Journal of Biological Chemistry*, vol. 254, pp. 10896-10900, 1979.
- [24] A. A. Farooqui and L. a Horrocks, "Plasmalogens, phospholipase A2, and docosahexaenoic acid turnover in brain tissue", *Journal of Molecular Neuroscience : MN*, vol. 16, no. 2-3, pp. 263-272, 2001.
- [25] H. Yang, A. A. Farooqui, and L. A. Horrocks, "Plasmalogen-selective phospholipase A2 and its role in signal transduction," *Journal of Lipid Mediators and Cell Signaling*, vol. 14, pp. 9-13, 1996.
- [26] D. A. Ford and R. W. Gross, "Plasmenylethanolamine is the major storage depot for arachidonic acid in rabbit vascular smooth muscle and is rapidly hydrolyzed after angiotensin II stimulation", *Proceedings of the National Academy of Sciences of the United States of America*, vol. 86, no. 10, pp. 3479-3483, 1989.
- [27] L. J. Pike, "Lipid rafts: bringing order to chaos", *Journal of Lipid Research*, vol. 44, no. 4, pp. 655-667, 2003.
- [28] L. J. Pike, X. Han, K.-N. Chung, and R. W. Gross, "Lipid rafts are enriched in arachidonic acid and plasmenylethanolamine and their composition is independent of caveolin-1

- expression: a quantitative electrospray ionization/mass spectrometric analysis”, *Biochemistry*, vol. 41, no. 6, pp. 2075–2088, 2002.
- [29] R. A. Zoeller, O. H. Morand, and C. R. Raetz, “A Possible Role for Plasmalogens in Protecting Animal Cells against Photosensitized killing”, *The Journal of Biological Chemistry*, vol. 263, no. 23, pp. 11590–11596, 1988.
- [30] H. K. Mangold and N. Weber, “Biosynthesis and biotransformation of ether lipids”, *Lipids*, vol. 22, pp. 789–799, 1987.
- [31] G. Hoefler, E. Paschke, S. Hoefler, a B. Moser, and H. W. Moser, “Photosensitized killing of cultured fibroblasts from patients with peroxisomal disorders due to pyrene fatty acid-mediated ultraviolet damage”, *The Journal of Clinical Investigation*, vol. 88, no. 6, pp. 1873–1879, 1991.
- [32] A. Dudda, G. Spiteller, and F. Kobelt, “Lipid oxidation products in ischemic porcine heart tissue”, *Chemistry and Physics of Lipids*, vol. 82, pp. 39–51, 1996.
- [33] P. Brites, R. J. Wanders, and H. R. Waterham, “The mouse as a model to understand peroxisomal biogenesis and its disorders”, *Drug Discovery Today: Disease Models*, vol. 1, no. 3, pp. 193–198, 2004.
- [34] C. Rodemer, T.-P. Thai, B. Brugger, T. Kaercher, H. Werner, K.-A. Nave, F. Wieland, K. Gorgas, and W. W. Just, “Inactivation of ether lipid biosynthesis causes male infertility, defects in eye development and optic nerve hypoplasia in mice”, *Human Molecular Genetics*, vol. 12, no. 15, pp. 1881–1895, 2003.
- [35] P. Brites, A. M. Motley, P. Gressens, P. a W. Mooyer, I. Ploegaert, V. Everts, P. Evrard, P. Carmeliet, M. Dewerchin, L. Schoonjans, M. Duran, H. R. Waterham, R. J. a Wanders, and M. Baes, “Impaired neuronal migration and endochondral ossification in Pex7 knockout mice: a model for rhizomelic chondrodysplasia punctata”, *Human Molecular Genetics*, vol. 12, no. 18, pp. 2255–2267, 2003.
- [36] P. Brites, P. Mooyer, L. Mrabet, H. Waterham, and R. Wanders, “Plasmalogens participate in very-long-chain fatty acid-induced pathology.,” *Brain: a journal of neurology*, vol. 132, pp. 482–92, Feb. 2009.
- [37] R. J. a Wanders and H. R. Waterham, “Peroxisomal disorders I: biochemistry and genetics of peroxisome biogenesis disorders” *Clinical Genetics*, vol. 67, no. 2, pp. 107–133, 2004.
- [38] S. Weller, S. J. Gould, and D. Valle, “Peroxisome biogenesis disorders”, *Annual Review of Genomics and Human Genetics*, vol. 4, pp. 165–211, 2003.
- [39] J. M. Nuoffer, J. P. Pfammatter, A. Spahr, H. Toplak, R. J. Wanders, R. B. Schutgens, and U. N. Wiesmann, “Chondrodysplasia punctata with a mild clinical course”, *Journal of Inherited Metabolic Disease*, vol. 17, pp. 60–66, 1994.
- [40] J. C. Heikoop, R. J. Wanders, A. Strijland, R. Purvis, R. B. Schutgens, and J. M. Tager, “Genetic and biochemical heterogeneity in patients with the rhizomelic form of chondrodysplasia punctata - a complementation study”, *Human Genetics*, vol. 89, pp. 439–44, 1992.
- [41] A. Poulos, L. Sheffield, P. Sharp, G. Sherwood, D. Johnson, K. Beckman, A. J. Fellenberg, J. E. Wraith, C. W. Chow, and S. Usher, “Rhizomelic chondrodysplasia punctata: clinical,

References

- pathologic, and biochemical findings in two patients,” *Journal of Pediatrics*, vol. 113, pp. 685–690, 1988.
- [42] R. G. F. Gray, S. Chapman, C. McKeown, R. B. H. Schutgens, and R. J. A. Wanders, “Rhizomelic chondrodysplasia punctata - A new clinical variant”, *Journal of Inherited Metabolic Disease*, vol. 15, pp. 931–932, 1992.
- [43] L. S. Sztriha, M. P. Nork, Y. M. Abdulrazzaq, L. I. Al-Gazali, and D. B. Bakalinova, “Abnormal myelination in peroxisomal isolated dihydroxyacetonephosphate acyltransferase deficiency”, vol. 16, no. 3. pp. 232–236, 1997.
- [44] L. Sztriha, L. I. Al-Gazali, R. J. Wanders, R. Ofman, M. P. Nork, and G. G. Lestringant, “Abnormal myelin formation in rhizomelic chondrodysplasia punctata type 2 (DHAPAT-deficiency)”, vol. 42. pp. 492–495, 2000.
- [45] A. M. Motley, P. Brites, L. Gerez, E. Hogenhout, J. Haasjes, R. Benne, H. F. Tabak, R. J. a Wanders, and H. R. Waterham, “Mutational spectrum in the PEX7 gene and functional analysis of mutant alleles in 78 patients with rhizomelic chondrodysplasia punctata type 1”, *American Journal of Human Genetics*, vol. 70, pp. 612–624, 2002.
- [46] A. M. Motley, E. H. Hetteema, E. M. Hogenhout, P. Brites, A. L. Asbroek, F. A. Wijburg, F. Baas, H. S. Heijmans, H. F. Tabak, R. J. A. Wanders, and B. Distel, “Rhizomelic chondrodysplasia punctata is a peroxisomal protein protein targeting disease caused by a non-functional PTS-2 receptor”, *Nature Genetics*, vol. 15, pp. 377–380, 1997.
- [47] P. E. Purdue, J. W. Zhang, M. Skoneczny, and P. B. Lazarow, “Rhizomelic chondrodysplasia punctata is caused by deficiency of human PEX7, a homologue of the yeast PTS2 receptor”, *Nature Genetics*, vol. 15, pp. 381–384, 1997.
- [48] A. W. Schram, S. Goldfischer, C. W. van Roermund, E. M. Brouwer-Kelder, J. Collins, T. Hashimoto, H. S. Heymans, H. van den Bosch, R. B. Schutgens, J. M. Tager, and R. J. Wanders, “Human peroxisomal 3-oxoacyl-coenzyme A thiolase deficiency,” *Proceedings of the National Academy of Sciences of the United States of America*, vol. 84, pp. 2494–2496, 1987.
- [49] J. C. Heikoop, C. W. T. Roermund, W. W. Just, R. Ofman, R. B. H. Schutgens, H. S. A. Heymans, R. J. Wanders, and J. M. Tager, “Rhizomelic Chondrodysplasia Punctata - Deficiency of 3-Oxoacyl-CoA thiolase in peroxisomes and impaired processing of the enzyme”, *Journal of Clinical Investigation*, vol. 86, pp. 126–130, 1990.
- [50] E. C. De Vet and H. Van Den Bosch, “Alkyl-dihydroxyacetonephosphate synthase”, *Cell Biochemistry and Biophysics*, vol. 1348, no. 1–2, pp. 117–121, 2000.
- [51] E. C. De Vet, L. Ijlst, W. Oostheim, C. Dekker, H. W. Moser, H. Van Den Bosch, and R. J. Wanders, “Ether lipid biosynthesis: alkyl-dihydroxyacetonephosphate synthase protein deficiency leads to reduced dihydroxyacetonephosphate acyltransferase activities”, *Journal of Lipid Research*, vol. 40, no. 11, pp. 1998–2003, 1999.
- [52] R. Ofman, E. H. Hetteema, E. M. Hogenhout, U. Caruso, a O. Muijsers, and R. J. Wanders, “Acyl-CoA:dihydroxyacetonephosphate acyltransferase: cloning of the human cDNA and resolution of the molecular basis in rhizomelic chondrodysplasia punctata type 2”, *Human Molecular Genetics*, vol. 7, no. 5, pp. 847–853, 1998.
- [53] R. J. Wanders, C. Dekker, V. A. Hovarth, R. B. Schutgens, J. M. Tager, P. Van Laer, and D. Lecoutere, “Human alkyl-dihydroxyacetonephosphate synthase deficiency: a new

- peroxisomal disorder”, *Journal of Inherited Metabolic Disease*, vol. 17, pp. 315–318, 1994.
- [54] E. C. J. M. de Vet, L. Ijlst, W. Oostheim, R. J. A. Wanders, and H. V. D. Bosch, “Alkyl-Dihydroxyacetonephosphate Synthase: Fate in peroxisome biogenesis disorders and identification of the point mutation underlying a single enzyme deficiency” *The Journal of Biological Chemistry*, vol. 273, no. 17, pp. 10296–10301, 1998.
- [55] L. Ginsberg, S. Rafique, J. H. Xuereb, S. I. Rapoport, and N. L. Gershfeld, “Disease and anatomic specificity of ethanolamine plasmalogen deficiency in Alzheimer’s disease brain,” *Brain Research*, vol. 698, pp. 223–226, 1995.
- [56] J. Kou, G. G. Kovacs, R. Höftberger, W. Kulik, A. Brodde, S. Forss-Petter, S. Hönigschnabl, A. Gleiss, B. Brügger, R. Wanders, W. Just, H. Budka, S. Jungwirth, P. Fischer, and J. Berger, “Peroxisomal alterations in Alzheimer’s disease”, *Acta Neuropathologica*, vol. 122, no. 3, pp. 271–283, 2011.
- [57] P. G. Pentchev, M. E. Comly, H. S. Kruth, M. T. Vanier, D. a Wenger, S. Patel, and R. O. Brady, “A defect in cholesterol esterification in Niemann-Pick disease (type C) patients”, *Proceedings of the National Academy of Sciences of the United States of America*, vol. 82, pp. 8247–8251, 1985.
- [58] S. Schedin, P. J. Sindelar, P. Pentchev, U. Brunk, and G. Dallner, “Peroxisomal impairment in Niemann-Pick type C disease”, *The Journal of Biological Chemistry*, vol. 272, pp. 6245–6251, 1997.
- [59] N. Braverman, R. Zhang, L. Chen, G. Nimmo, S. Scheper, T. Tran, R. Chaudhury, A. Moser, and S. Steinberg, “A Pex7 hypomorphic mouse model for plasmalogen deficiency affecting the lens and skeleton”, *Molecular Genetics and Metabolism*, vol. 99, no. 4, pp. 408–416, 2010.
- [60] R. Liegel, B. Chang, R. Dubielzig, and D. J. Sidjanin, “Blind sterile 2 (bs2), a hypomorphic mutation in Agps, results in cataracts and male sterility in mice”, *Molecular Genetics and Metabolism*, vol. 103, no. 1, pp. 51–59, 2011.
- [61] K. R. Jessen, “Glial cells”, *The International Journal of Biochemistry & Cell Biology*, vol. 36, pp. 1861–1867, 2004.
- [62] B. Garbay, A. M. Heape, F. Sargueil, and C. Cassagne, “Myelin synthesis in the peripheral nervous system”, *Progress in Neurobiology*, vol. 61, no. 3, pp. 267–304, 2000.
- [63] N. Le Douarin, C. Dulac, E. Dupin, and P. Cameron-Curry, “Glial cell lineages in the neural crest”, *Glia*, vol. 4, no. 2, pp. 175–184, 1991.
- [64] K. R. Jessen and R. Mirsky, “Schwann cells and their precursors emerge as major regulators of nerve development”, *Trends in Neurosciences*, vol. 22, no. 9, pp. 402–410, 1999.
- [65] R. Mirsky, A. Woodhoo, D. B. Parkinson, P. Arthur-farraj, A. Bhaskaran, and K. R. Jessen, “Novel signals controlling embryonic Schwann cell development , myelination and dedifferentiation”, *Journal of Peripheral Nervous System*, vol. 135, pp. 122–135, 2008.
- [66] J. L. Salzer and R. P. Bunge, “Studies of Schwann cell proliferation. I. An analysis in tissue culture of proliferation during development, Wallerian degeneration, and direct injury”, *The Journal of Cell Biology*, vol. 84, no. 3, pp. 739–752, 1980.

References

- [67] S. Poliak and E. Peles, "The local differentiation of myelinated axons at nodes of Ranvier" *Nature reviews. Neuroscience*, vol. 4, no. 12, pp. 968–980, 2003.
- [68] S. G. Waxman and T. J. Sims, "Specificity in central myelination: evidence for local regulation of myelin thickness", *Brain Research*, vol. 292, no. 1, pp. 179–185, 1984.
- [69] R. P. Bunge, M. B. Bunge, and M. Bates, "Movements of the Schwann cell nucleus implicate progression of the inner (axon-related) Schwann cell process during myelination", *The Journal of Cell Biology*, vol. 109, no. 1, pp. 273–284, 1989.
- [70] F. Eldridge, M. B. Bungs, and R. P. Bunge, "Differentiation of Axon-Related Schwann Cells *in vitro*: II . Control of Myelin Formation by Basal Lamina", vol. 9, pp. 625–638, 1989.
- [71] C. F. Eldridge, M. B. Bunge, R. P. Bunge, and P. M. Wood, "Differentiation of axon-related Schwann cells *in vitro*. I. Ascorbic acid regulates basal lamina assembly and myelin formation", *The Journal of Cell Biology*, vol. 105, no. 2, pp. 1023–1034, 1987.
- [72] K.-A. Nave and J. L. Salzer, "Axonal regulation of myelination by neuregulin 1", *Current Opinion in Neurobiology*, vol. 16, no. 5, pp. 492–500, 2006.
- [73] K. Hirata and M. Kawabuchi, "Myelin phagocytosis by macrophages and nonmacrophages during Wallerian degeneration", *Microscopy Research and Technique*, vol. 57, no. 6, pp. 541–547, 2002.
- [74] M. C. Harrisingh, E. Perez-Nadales, D. B. Parkinson, D. S. Malcolm, A. W. Mudge, and A. C. Lloyd, "The Ras/Raf/ERK signalling pathway drives Schwann cell dedifferentiation", *The EMBO Journal*, vol. 23, no. 15, pp. 3061–3071, 2004.
- [75] S. G. Waxman and J. M. Ritchie, "Molecular dissection of the myelinated axon", *Annals of Neurology*, vol. 33, no. 2, pp. 121–136, 1993.
- [76] E. Kordeli, S. Lambert, and V. Bennett, "A new ankyrin gene with neural-specific isoforms localized at the axonal initial segment and node of Ranvier", *The Journal of Biological Chemistry*, vol. 270, no. 5, pp. 2352–2359, 1995.
- [77] S. Berghs, D. Aggujaro, R. Dirx, E. Maksimova, P. Stabach, J.-M. Hermel, J.-P. Zhang, W. Philbrick, V. Slepnev, T. Ort, and M. Solimena, "betaIV spectrin, a new spectrin localized at axon initial segments and nodes of ranvier in the central and peripheral nervous system", *The Journal of Cell Biology*, vol. 151, no. 5, pp. 985–1002, 2000.
- [78] H. J. Bellen, Y. Lu, R. Beckstead, and M. a Bhat, "Neurexin IV, caspr and paranodin - novel members of the neurexin family: encounters of axons and glia", *Trends in Neurosciences*, vol. 21, no. 10, pp. 444–449, 1998.
- [79] J. L. Salzer, "Polarized domains of myelinated axons", *Neuron*, vol. 40, no. 2, pp. 297–318, 2003.
- [80] F. A. Court, J. Hewitt, K. Davies, B. L. Patton, A. Uncini, L. Wrabetz, and M. L. Feltri, "A Laminin-2, Dystroglycan, Utrophin Axis Is Required for Compartmentalization and Elongation of Myelin Segments", *The Journal of Neuroscience*, vol. 29, no. 12, pp. 3908–3919, 2009.
- [81] K. Matsumura, H. Yamada, T. Shimizu, and K. P. Campbell, "Differential expression of dystrophin, utrophin and dystrophin-associated proteins in peripheral nerve", *FEBS letters*, vol. 334, no. 3, pp. 281–285, 1993.

- [82] Y.-J. Chen, H. J. Spence, J. M. Cameron, T. Jess, J. L. Ilsley, and S. J. Winder, "Direct interaction of beta-dystroglycan with F-actin", *The Biochemical Journal*, vol. 375, no. 2, pp. 329–337, 2003.
- [83] T. Masaki and K. Matsumura, "Biological Role of Dystroglycan in Schwann Cell Function and Its Implications in Peripheral Nervous System Diseases", *Journal of Biomedicine Biotechnology*, vol. 2010, p. 740403, 2010.
- [84] F. A. Court, D. Zambroni, E. Pavoni, C. Colombelli, C. Baragli, G. Figlia, L. Sorokin, W. Ching, J. L. Salzer, L. Wrabetz, and M. L. Feltri, "MMP2-9 Cleavage of Dystroglycan Alters the Size and Molecular Composition of Schwann Cell Domains", *The Journal of Neuroscience the Official Journal of the Society for Neuroscience*, vol. 31, no. 34, pp. 12208–12217, 2011.
- [85] K.-A. Nave and B. D. Trapp, "Axon-glia signaling and the glial support of axon function", *Annual Review of Neuroscience*, vol. 31, pp. 535–561, 2008.
- [86] C. Birchmeier and K.-A. Nave, "Neuregulin-1, a key axonal signal that drives Schwann cell growth and differentiation", *Glia*, vol. 56, no. 14, pp. 1491–1497, 2008.
- [87] G. V. Michailov, M. W. Sereida, B. G. Brinkmann, T. M. Fischer, B. Haug, C. Birchmeier, L. Role, C. Lai, M. H. Schwab, and K.-A. Nave, "Axonal neuregulin-1 regulates myelin sheath thickness", *Science New York NY*, vol. 304, no. 5671, pp. 700–703, 2004.
- [88] J. A. Pereira, F. Lebrun-Julien, and U. Suter, "Molecular mechanisms regulating myelination in the peripheral nervous system", *Trends in Neurosciences*, vol. 35, no. 2, pp. 123–134, 2011.
- [89] T. Ogata, S. Iijima, S. Hoshikawa, T. Miura, S. Yamamoto, H. Oda, K. Nakamura, and S. Tanaka, "Opposing extracellular signal-regulated kinase and Akt pathways control Schwann cell myelination", *The Journal of Neuroscience*, vol. 24, no. 30, pp. 6724–6732, 2004.
- [90] L. Cotter, M. Özçelik, C. Jacob, J. A. Pereira, V. Locher, R. Baumann, J. B. Relvas, U. Suter, and N. Tricaud, "Dlg1-PTEN interaction regulates myelin thickness to prevent damaging peripheral nerve overmyelination", *Science New York NY*, vol. 328, no. 5984, pp. 1415–1418, 2010.
- [91] S.-C. Kao, H. Wu, J. Xie, C.-P. Chang, J. A. Ranish, I. A. Graef, and G. R. Crabtree, "Calcineurin/NFAT signaling is required for neuregulin-regulated Schwann cell differentiation", *Science New York NY*, vol. 323, no. 5914, pp. 651–654, 2009.
- [92] Y. He, J. Y. Kim, J. Dupree, A. Tewari, C. Melendez-Vasquez, J. Svaren, and P. Casaccia, "Yy1 as a molecular link between neuregulin and transcriptional modulation of peripheral myelination" *Nature Neuroscience*, vol. 13, no. 12, pp. 1472–1480, 2010.
- [93] J. Svaren and D. Meijer, "The molecular machinery of myelin gene transcription in Schwann cells" *Glia*, vol. 56, no. 14, pp. 1541–1551, 2008.
- [94] C. M. Kassmann, C. Lappe-Siefke, M. Baes, B. Brügger, A. Mildner, H. B. Werner, O. Natt, T. Michaelis, M. Prinz, J. Frahm, and K.-A. Nave, "Axonal loss and neuroinflammation caused by peroxisome-deficient oligodendrocytes", *Nature Genetics*, vol. 39, no. 8, pp. 969–976, 2007.
- [95] M. Baarine, K. Ragot, E. C. Genin, H. El Hajj, D. Trompier, P. Andreoletti, M. S. Ghandour, F. Menetrier, M. Cherkaoui-Malki, S. Savary, and G. Lizard, "Peroxisomal and

References

- mitochondrial status of two murine oligodendrocytic cell lines (158N, 158JP): potential models for the study of peroxisomal disorders associated with dysmyelination processes”, *Journal of Neurochemistry*, vol. 111, no. 1, pp. 119–131, 2009.
- [96] M. O. W. Grimm, J. Kuchenbecker, T. L. Rothhaar, S. Grösgen, B. Hundsdörfer, V. K. Burg, P. Friess, U. Müller, H. S. Grimm, M. Riemenschneider, and T. Hartmann, “Plasmalogen synthesis is regulated via alkyl-dihydroxyacetonephosphate-synthase by amyloid precursor protein processing and is affected in Alzheimer’s disease”, *Journal of Neurochemistry*, vol. 116, no. 5, pp. 916–925, 2011.
- [97] B. Itzkovitz, S. Jiralerspong, G. Nimmo, M. Loscalzo, D. D. G. Horovitz, A. Snowden, A. Moser, S. Steinberg, and N. Braverman, “Functional characterization of novel mutations in GNPAT and AGPS, causing rhizomelic chondrodysplasia punctata (RCDP) types 2 and 3”, *Human Mutation*, vol. 33, no. 1, pp. 189–197, 2012.
- [98] T. F. Silva, J. Eira, A. T. Lopes, V. F. Sousa, A. R. Malheiro, A. Luoma, R. Wanders, D. A. Kirschner, M. M. Sousa, and P. Brites, “Ether-phospholipids regulate axonal sorting, myelination and regeneration by impairing AKT activation. Manuscript in preparation”, 2012.
- [99] R. J. Balice-Gordon, L. J. Bone, and S. S. Scherer, “Functional gap junctions in the schwann cell myelin sheath”, *The Journal of Cell Biology*, vol. 142, no. 4, pp. 1095–1104, 1998.
- [100] B. L. Berger and R. Gupta, “Demyelination secondary to chronic nerve compression injury alters Schmidt-Lanterman incisures” *Journal of Anatomy*, vol. 209, no. 1, pp. 111–118, 2006.
- [101] A. Kun, L. Canclini, G. Rosso, M. Bresque, C. Romeo, A. Hanusz, K. Cal, A. Calliari, J. Sotelo Silveira, and J. R. Sotelo, “F-actin distribution at nodes of Ranvier and Schmidt-Lanterman incisures in mammalian sciatic nerves”, *Cytoskeleton*, pp. 1–10, 2012.
- [102] P. Maurel, S. Einheber, J. Galinska, P. Thaker, I. Lam, M. B. Rubin, S. S. Scherer, Y. Murakami, D. H. Gutmann, and J. L. Salzer, “Nectin-like proteins mediate axon-Schwann cell interactions along the internode and are essential for myelination”, *The Journal of Cell Biology*, vol. 178, no. 5, pp. 861–874, 2007.
- [103] S. Päiväläinen, M. Nissinen, H. Honkanen, O. Lahti, S. M. Kangas, J. Peltonen, S. Peltonen, and A. M. Heape, “Myelination in mouse dorsal root ganglion/Schwann cell cocultures”, *Molecular and Cellular Neuroscience*, vol. 37, no. 3, pp. 568–578, 2008.
- [104] W.-L. Yang, J. Wang, C.-H. Chan, S.-W. Lee, A. D. Campos, B. Lamothe, L. Hur, B. C. Grabiner, X. Lin, B. G. Darnay, and H.-K. Lin, “The E3 ligase TRAF6 regulates Akt ubiquitination and activation”, *Science (New York, N.Y.)*, vol. 325, no. 5944, pp. 1134–1138, 2009.
- [105] K. M. Nicholson and N. G. Anderson, “The protein kinase B/Akt signalling pathway in human malignancy”, *Cellular Signalling*, vol. 14, no. 5, pp. 381–395, 2002.
- [106] R. J. Baldessarini, L. Tondo, P. Davis, M. Pompili, F. K. Goodwin, and J. Hennen, “Decreased risk of suicides and attempts during long-term lithium treatment: a meta-analytic review”, *Bipolar Disorders*, vol. 8, no. 5 Pt 2, pp. 625–639, 2006.
- [107] P. S. Klein and D. a Melton, “A molecular mechanism for the effect of lithium on development”, *Proceedings of the National Academy of Sciences of the United States of America*, vol. 93, no. 16, pp. 8455–8459, 1996.

- [108] J. a Quiroz, R. Machado-Vieira, C. a Zarate, and H. K. Manji, "Novel insights into Lithium's mechanism of action: neurotrophic and neuroprotective effects", *Neuropsychobiology*, vol. 62, no. 1, pp. 50-60, 2010.
- [109] A. Mora, G. Sabio, A. M. Risco, A. Cuenda, J. C. Alonso, G. Soler, and F. Centeno, "Lithium blocks the PKB and GSK3 dephosphorylation induced by ceramide through protein phosphatase-2A", *Cellular Signalling*, vol. 14, no. 6, pp. 557-562, 2002.
- [110] B. D. Manning and L. C. Cantley, "Akt/PKB Signaling", *Cell*, vol. 129, no. 2003, 2007.
- [111] S. Zimmermann and K. Moelling, "Phosphorylation and regulation of Raf by Akt (protein kinase B)" *Science New York NY*, vol. 286, no. 5445, pp. 1741-1744, 1999.
- [112] P. Brites, A. S. Ferreira, T. F. da Silva, V. F. Sousa, A. R. Malheiro, M. Duran, H. R. Waterham, M. Baes, and R. J. a Wanders, "Alkyl-glycerol rescues plasmalogen levels and pathology of ether-phospholipid deficient mice", *PloS One*, vol. 6, no. 12, p. e28539, 2011.
- [113] N. B. Jagalur, M. Ghazvini, W. Mandemakers, S. Driegen, A. Maas, E. A. Jones, M. Jaegle, F. Grosveld, J. Svaren, and D. Meijer, "Functional dissection of the Oct6 Schwann cell enhancer reveals an essential role for dimeric Sox10 binding", *The Journal of Neuroscience the Official Journal of the Society for Neuroscience*, vol. 31, no. 23, pp. 8585-8594, 2011.

